We also investigated the signal transduction pathways involved in BTC auto- and cross-induction. Western blot analysis showed that BTC activates ErbB1 in NHEK (Fig. 2A). A previous report showed that BTC activates mitogen activated protein kinase (MAPK). We examined whether BTC activates MAPK proteins in NHEK. BTC stimulated the phosphorylation of MAPK proteins including extracellular signal-regulated kinase (ERK), p38, and c-Jun N-terminal kinase (JNK) in NHEK (Fig. 2B). To examine which pathways might be involved in auto- and cross-induction, we used specific inhibitors of ErbB1, MAKP/ERK kinase (MEK, upstream of ERK), p38 and JNK. Treatment with the ErbB1 inhibitor completely blocked the induction of BTC, as well as other EGF family members, while treatment with the JNK and MEK inhibitors suppressed their expression (Fig. 2C). By contrast, the p38 inhibitor did not affect the induction of EGF family members by BTC (Fig. 2C). These results indicate that BTC induces auto- and cross-induction through the activation of ErbB1, MEK-ERK, and JNK signaling. The effect of MEK inhibitor is less effective than ErbB1 inhibitor or JNK inhibitor. Because knockout of MAPK pathways leads to distinct phenotypes in mice [5], the differences of the effects on auto- and cross-induction may be due to their specific non-redundant biological functions.

This study directly demonstrates that BTC, like HB-EGF, AREG, TGF-α and EREG, is an autocrine growth factor in NHEK. All EGF family members that bind ErbB1 promote NHEK growth. However, they each have their own distinct biological functions. Loss of TGF-α *in vivo* results in the retardation of partial thickness wound healing. In keratinocyte-specific HB-EGF knockout mice, the migration but not proliferation of wound edge keratinocytes was impaired [6]. Loss of other EGF family members causes no obvious skin phenotype in mice. AREG-transgenic mice exhibited a severe inflammatory and hyperproliferative psoriatic phenotype, while TGF-α overexpression causes epidermal thickening [7,8]. By contrast, BTC-transgenic mice showed increased keratinocyte proliferation, a significant delay in hair follicle morphogenesis, and enhanced wound healing-associated angiogenesis [9]. Immunohistochemical staining revealed that HB-EGF was diffusely expressed throughout normal and psoriatic epidermis, whereas BTC was largely restricted to the spinous and granular layer [10]. These findings suggest that BTC, like other autocrine growth factors, may have a distinct, non-redundant biological function in normal human skin.

We have shown that BTC induces its own expression, as well as that of other EGF family members, and that other EGF family members induce BTC expression. Auto- and cross-regulatory mechanisms may be very effective in stimulating keratinocyte proliferation, but problematic when the aim is to arrest tumor cell growth. We clearly demonstrated that auto- and cross-induction are mediated through ErbB1, MEK-ERK, and JNK pathways. Numerous ErbB blockers have been tested as possible suppressors of tumor growth and some, including anti-ErbB1 monoclonal antibodies and tyrosine kinase inhibitors, are now being used clinically [2]. Therapeutic strategies targeting MEK-ERK or JNK, meanwhile, may produce beneficial anti-proliferative effects in hyperproliferative disorders of the epidermis.

In this study, we demonstrate that BTC is an autocrine growth factor in NHEK and that auto- and cross-induction of EGF family members by BTC is mediated by the ERK and JNK signaling pathways.

Acknowledgements

This work was supported by a Grant-in-aid for Scientific Research from the Ministry of Education, Science, Culture and Sports of Japan, and by Health and Labour Sciences Research Grants (Research on Intractable Diseases) from the Ministry of Health, Labour and Welfare of Japan.

References

[1] Hashimoto K. Regulation of keratinocyte function by growth factors. J Dermatol Sci 2000;24(Suppl 1):S46–50.
[2] Kataoka H. EGFR ligands and their signaling scissors, ADAMs, as new molecular targets for anticancer treatments. J Dermatol Sci 2009;56:148–53.
[3] Shirakata Y, Komurasaki T, Toyoda H, Hanakawa Y, Yamasaki K, Tokumaru S, et al. a novel member of the epidermal growth factor family, is an autocrine growth factor in normal human keratinocytes. J Biol Chem 2000;275:5748–53.
[4] Dunbar AJ, Goddard C. Structure-function and biological role of betacellulin. Int J Biochem Cell Biol 2000;32:805–15.
[5] Aouadi M, Binetruy B, Caron L, Le Marchand-Brustel Y, Bost F. Role of MAPKs in development and differentiation: lessons from knockout mice. Biochimie 2006;88:1091–8.
[6] Shirakata Y, Kimura R, Nanba D, et al. Heparin-binding EGF-like growth factor accelerates keratinocyte migration and skin wound healing. J Cell Sci 2005;118:2363–70.
[7] Cook PW, Piepkorn M, Clegg CH, Plowman GD, DeMay JM, Brown JR, et al. Transgenic expression of the human amphiregulin gene induces a psoriasis-like phenotype. J Clin Invest 1997;100:2286–94.
[8] Vassar R, Fuchs E. Transgenic mice provide new insights into the role of TGF-alpha during epidermal development and differentiation. Genes Dev 1991;5: 714–27.
[9] Schneider MR, Antsiferova M, Feldmeyer L, Dahlhoff M, Bugnon P, Hasse S, et al. Betacellulin regulates hair follicle development and hair cycle induction and enhances angiogenesis in wounded skin. J Invest Dermatol 2008;128:1256–65.
[10] Piepkorn M, Predd H, Underwood R, Cook P. Proliferation-differentiation relationships in the expression of heparin-binding epidermal growth factor-related factors and erbB receptors by normal and psoriatic human keratinocytes. Arch Dermatol Res 2003;295:93–101.

Yuji Shirakata*
Sho Tokumaru
Koji Sayama
Koji Hashimoto
Department of Dermatology, Ehime University Graduate School of Medicine, Shitsukawa, Toon, Ehime 791-0295, Japan
*Corresponding author. Tel.: +81 89 960 5350; fax: +81 89 960 5352

E-mail address: shirakat@m.ehime-u.ac.jp (Y. Shirakata)

4 March 2010

doi:10.1016/j.jdermsci.2010.03.016

OPEN ACCESS Freely available online

PLoS one

Inflammatory Mediator TAK1 Regulates Hair Follicle Morphogenesis and Anagen Induction Shown by Using Keratinocyte-Specific TAK1-Deficient Mice

Koji Sayama[1]*, Kentaro Kajiya[2], Koji Sugawara[3], Shintaro Sato[4], Satoshi Hirakawa[1], Yuji Shirakata[1], Yasushi Hanakawa[1], Xiuju Dai[1], Yumiko Ishimatsu-Tsuji[2], Daniel Metzger[5], Pierre Chambon[5], Shizuo Akira[6], Ralf Paus[3,7], Jiro Kishimoto[2], Koji Hashimoto[1]

1 Department of Dermatology, Ehime University Graduate School of Medicine, Ehime, Japan, 2 Skin Biology Research Group, Shiseido Innovative Science Research and Development Center, Yokohama, Japan, 3 Department of Dermatology, University of Luebeck, Luebeck, Germany, 4 Department of Microbiology and Immunology, The Institute of Medical Science, The University of Tokyo, Tokyo, Japan, 5 Institut de Génétique et de Biologie Moléculaire et Cellulaire (IGBMC), CNRS, INSERM, UdS, Collège de France, Illkirch, France, 6 Research Institute for Microbial Disease, Osaka University, Suita, Japan, 7 School of Translational Medicine, University of Manchester, Manchester, United Kingdom

Abstract

Transforming growth factor-β-activated kinase 1 (TAK1) is a member of the NF-κB pathway and regulates inflammatory responses. We previously showed that TAK1 also regulates keratinocyte growth, differentiation, and apoptosis. However, it is unknown whether TAK1 has any role in epithelial–mesenchymal interactions. To examine this possibility, we studied the role of TAK1 in mouse hair follicle development and cycling as an instructive model system. By comparing keratinocyte-specific TAK1-deficient mice (*Map3k7*$^{fl/fl}$K5-Cre) with control mice, we found that the number of hair germs (hair follicles precursors) in *Map3k7*$^{fl/fl}$K5-Cre mice was significantly reduced at E15.5, and that subsequent hair follicle morphogenesis was retarded. Next, we analyzed the role of TAK1 in the cyclic remodeling in follicles by analyzing hair cycle progression in mice with a tamoxifen-inducible keratinocyte-specific TAK1 deficiency (*Map3k7*$^{fl/fl}$K14-Cre-ER^{T2}). After active hair growth (anagen) was induced by depilation, TAK1 was deleted by topical tamoxifen application. This resulted in significantly retarded anagen development in TAK1-deficient mice. Deletion of TAK1 in hair follicles that were already in anagen induced premature, apoptosis-driven hair follicle regression, along with hair follicle damage. These studies provide the first evidence that the inflammatory mediator TAK1 regulates hair follicle induction and morphogenesis, and is required for anagen induction and anagen maintenance.

Citation: Sayama K, Kajiya K, Sugawara K, Sato S, Hirakawa S, et al. (2010) Inflammatory Mediator TAK1 Regulates Hair Follicle Morphogenesis and Anagen Induction Shown by Using Keratinocyte-Specific TAK1-Deficient Mice. PLoS ONE 5(6): e11275. doi:10.1371/journal.pone.0011275

Editor: Vincent Laudet, Ecole Normale Supérieure de Lyon, France

Received March 19, 2010; **Accepted** May 30, 2010; **Published** June 23, 2010

Funding: This study was supported in part by grants from the Ministries of Education, Culture, Sports, Science, and Technology of Japan to K.S. and K.H., by Health and Labor Sciences Research Grants (Research on Intractable Diseases) from the Ministry of Health, Labor, and Welfare of Japan to K.H., by the Deutsche Forschungsgemeinschaft (DFG 345 Pa/12-2) to R.P., and by the College de France to P.C. The funders had no role in study design, data collection and analysis, decision to publish, or preparation of the manuscript.

Competing Interests: The authors have declared that no competing interests exist.

* E-mail: sayama@m.ehime-u.ac.jp

Introduction

The NF-κB pathway mediates innate immune or pro-inflammatory responses, such as signaling by Toll-like receptors (TLRs), the IL-1 receptor (IL-1R), and tumor necrosis factor receptor (TNFR) [1,2]. Transforming growth factor-β-activated kinase 1 (TAK1) is a member of the MAP3 kinase family [3] and an important member of the NK-κB pathway, involved in IL-1 and TNF-α-induced activation of NF-κB and MAP kinases [1]. Upon ligand binding, TNF-receptor-associated factor (TRAF) 6 or TRAF2 [4,5,6] activates TAK1, which then phosphorylates IκB kinases (IKKs), resulting in NF-κB activation.

Because members of the NF-κB pathway are increasingly recognized as important in the regulation of epithelial–mesenchymal interaction systems, ranging from tooth development to hair follicle induction and morphogenesis [7,8,9,10,11], we were interested in learning whether TAK1 also played a role in the biology of the hair follicle, a prototypic epithelial–mesenchymal interaction system. This interest was further fueled by our previous discovery in keratinocyte-specific TAK1-deficient mice (*Map3k7*$^{fl/fl}$K5-Cre) that TAK1 regulates keratinocyte growth, differentiation, and apoptosis [12]. However, the role of TAK1 in hair follicles has not been previously studied.

Induction and morphogenesis of the hair follicle [13] is controlled by complex signaling networks within the skin epithelium and between the epithelium and specialized inductive fibroblasts in its adjacent mesenchyme [7,11]. Among these signaling networks, the NF-κB pathway and Wnt/β-catenin signaling provide central controls [7,8]; however, the exact relationship between these signaling networks is not fully understood. Binding of EdaA1 to its receptor EdaR in the embryo is essential for the development of ectodermal appendages [14], and mutations in these genes cause reduced or absent ectodermal appendages [15,16,17,18,19]. Subsequently, the EdaA1/EdaR pathway activates the downstream NF-κB pathway [20]. A recent report showed that Wnt/β-catenin signaling lies both upstream

and downstream of the EdaR/NF-κB pathway [8]. Wnt/β-catenin signaling within the epithelial cells is required for activation of the Eda/EdaR/NF-κB pathway at an early stage of hair follicle development [8], and the expression of Eda and EdaR requires Wnt/β-catenin signaling [8]. At a later stage, maintenance of Wnt signaling and elevated Wnt10a, Wnt10b, and Dkk4 expression requires the Eda/EdaR/NF-κB pathway [8].

The postnatal hair cycle in mice begins with catagen induction around P17, followed by the first telogen. Recently, the EdaR pathway has been shown to be involved in the hair cycle [9,21,22]. The expression of EdaA1 and EdaR increases in the anagen-catagen phase [21]. Furthermore, EdaA1 prolongs the anagen phase [22]. Thus, in addition to its well-established role in hair follicle morphogenesis, the EdaR pathway is also involved in hair cycle control.

Since TAK1 is a member of NF-κB pathway, we hypothesized that TAK1 is involved in hair follicle morphogenesis and hair cycle control. To explore this, we studied hair follicle development in keratinocyte-specific TAK1-deficient (*Map3k7*$^{fl/fl}$K5-Cre) mice and subsequent hair follicle cycling in tamoxifen-inducible keratinocyte-specific TAK1 deficient mice (*Map3k7*$^{fl/fl}$K14-Cre-ER^{T2}) to avoid gene-targeting in embryonic development because this might damage the hair follicle, impairing its later capacity to cycle. These studies provide the first evidence that TAK1 regulates hair follicle induction, morphogenesis, and cycling.

Materials and Methods

Ethics Statement

The protocol for generating *Map3k7*$^{fl/fl}$K5-Cre mice and *Map3k7*$^{fl/fl}$K14-Cre-ER^{T2} mice was approved by the Institutional Review Board of Ehime University Graduate School of Medicine (#I-20-13 and #NE-27-16).

Generation of keratinocyte-specific TAK1-deficient mice (*Map3k7*$^{fl/fl}$ K5-Cre)

TAK1 is encoded by the *Map3k7* gene. The targeting construct has been described previously [1]. We generated keratinocyte-specific TAK1-deficient mice (*Map3k7*$^{fl/fl}$K5-Cre) by breeding *Map3k7*$^{fl/fl}$ mice (C57Bl/6 background) with K5-Cre mice (C57Bl/6 background) [23], as previously described [12].

Generation of tamoxifen-inducible keratinocyte-specific TAK1-deficient mice (*Map3k7*$^{fl/fl}$ K14-Cre-ER^{T2})

Map3k7K$^{fl/fl}$ mice were bred with K14-Cre-ER^{T2} mice (C57Bl/6 background) [24,25] to generate *Map3k7*$^{fl/fl}$K14-Cre-ER^{T2} mice. We applied 100 μL of 4-hydroxytamoxifen (Sigma-Aldrich Co., St. Louis, MO) in ethanol at a concentration of 1 mg/mL topically to the dorsal skin of 8-week-old female *Map3k7*$^{fl/fl}$K14-Cre-ER^{T2} mice for 5 consecutive days [24].

Wax depilation

The hair cycle was synchronized in the dorsal skin of 8-week-old female mice by wax (SURGI-WAX^{TM}, Ardell International, Los Angeles, CA) depilation, as described previously [26].

Histological analysis

The stages of hair follicle morphogenesis, cycling, and dystrophic catagen were morphologically defined using dorsal skin of the mice and the score was defined as follows.

The hair morphogenesis stage of each hair follicle in each mouse group was evaluated as described previously [13]. At least 40 hair follicles or all hair follicles in the mice were evaluated in each mouse group (two mice/group). The score of each hair morphogenesis stage was defined as follows: stage 1 = 1, stage 2 = 2, stage 3 = 3, stage 4 = 4, stage 5 = 5, stage 6 = 6, stage 7 = 7, and stage 8 = 8. Then, the rate (%) of a certain hair morphogenesis stage in the total hair follicles and the median score in each mouse group were determined. The score of *Map3k7*$^{fl/fl}$K5-Cre mice was compared with *Map3k7*$^{fl/fl}$ mice. Statistical significance was determined using a Mann-Whitney's U-test. A difference of $^{*}P<0.01$ was considered statistically significant.

The hair cycle stage of each hair follicle in each mouse group was evaluated as described previously [27]. At least 40 hair follicles were evaluated in each mouse group (two mice/group). The score of each hair cycle stage was defined as follows: catagen I = 1, catagen II = 2, catagen III = 3, catagen IV = 4, catagen V = 5, catagen VI = 6, catagen VII = 7, catagen VIII = 8, telogen = 9, anagen I = 10, anagen II = 11, anagen IIIa = 12, anagen IIIb = 13, anagen IIIc = 14, anagen IV = 15, anagen V = 16, and anagen VI = 17. Then, the rate (%) of a certain hair cycle stage in the total hair follicles and the median score in each mouse group were determined. The score of tamoxifen-treated *Map3k7*$^{fl/fl}$K14-Cre-ER^{T2} mice was compared with the control mice. Statistical significance was determined using a Mann-Whitney's U-test. A difference of $^{*}P<0.01$ was considered statistically significant.

Dystrophic catagen was defined according to a previous report [28] as early dystrophic catagen, mid dystrophic catagen, late dystrophic catagen, and dystrophic telogen. Then, the rate (%) of a certain hair follicle stage per total hair follicles was calculated in each mouse group. At least 40 hair follicles were evaluated in each mouse group (two mice/group).

Results

Impaired hair follicle morphogenesis in keratinocyte-specific TAK1-deficient mice

Keratinocyte-specific TAK1-deficient (*Map3k7*$^{fl/fl}$K5-Cre) mice were generated, as previously described [12]. *Map3k7*$^{fl/fl}$ mice were used as controls. Histological analysis of hair follicle development is shown in Figure 1A. Although hair germs (follicle precursors) and dermal condensations appeared in both types of mice at E15.5, the number of hair germs in *Map3k7*$^{fl/fl}$K5-Cre mice was significantly lower than that in *Map3k7*$^{fl/fl}$ mice (Fig. 1A). At E16.5, the hair germ further progressed into the hair peg stage of hair follicle morphogenesis in *Map3k7*$^{fl/fl}$ mice at the rate expected for wild-type mice [29], while hair pegs were essentially absent in *Map3k7*$^{fl/fl}$K5-Cre mice. Similarly, at P1-6, postnatal hair follicle development was severely impaired in *Map3k7*$^{fl/fl}$K5-Cre mice (Fig. 1A).

Hair follicle morphogenesis was quantitatively analyzed. The morphogenesis stage and the median score of each mouse group are shown in Fig. 1B. Hair follicle morphogenesis indicators were significantly delayed in *Map3k7*$^{fl/fl}$K5-Cre mice, as evident from their lower hair morphogenesis score, compared with *Map3k7*$^{fl/fl}$ mice at P3 and P6 (Fig. 1B).

Generation of tamoxifen-inducible keratinocyte-specific TAK1-deficient mice

Because germline targeting of TAK1 greatly disrupted hair morphogenesis and, thus, precluded a meaningful analysis of subsequent hair follicle cycling, we next used tamoxifen-inducible keratinocyte-specific TAK1-deficient mice (*Map3k7*$^{fl/fl}$K14-Cre-ER^{T2}), in which Cre-ER^{T2} was expressed in the epidermis under the control of the K14 promoter [24]. Southern blot analysis demonstrated efficient deletion of the floxed allele in the epidermis of tamoxifen-treated *Map3k7*$^{fl/fl}$K14-Cre-ER^{T2} mice (Fig. 2).

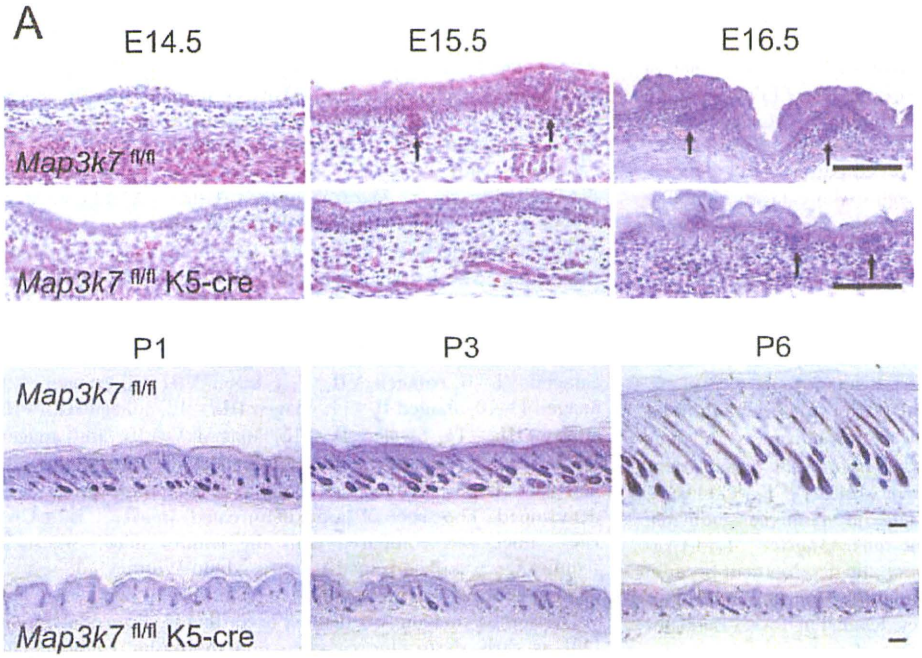

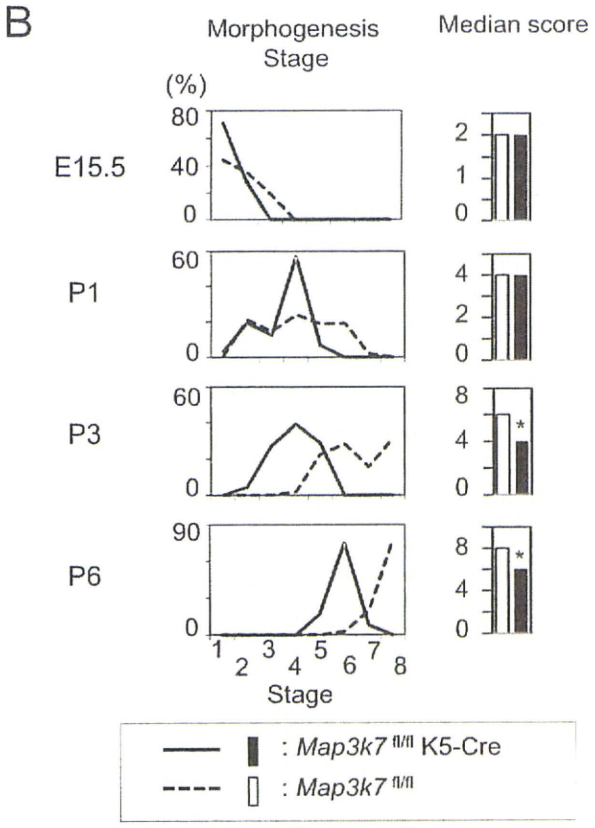

Figure 1. Impaired hair follicle morphogenesis in keratinocyte-specific TAK1-deficient mice. (A) Histological analysis of hair follicle development from E14.5 to P6. *Map3k7*$^{fl/fl}$K5-Cre were keratinocyte-specific TAK1-deficient mice [12]. *Map3k7*$^{fl/fl}$ mice were used as controls. Arrows indicate hair germs or hair pegs. Scale bar, 100 μm. (B) The hair morphogenesis stage of each hair follicle in each mouse group was evaluated as described previously [13]. Then, the rate (%) of a certain hair morphogenesis stage in the total hair follicles (left panel) and the median score in each mouse group (right panel) were determined. The score of *Map3k7*$^{fl/fl}$K5-Cre mice was compared with *Map3k7*$^{fl/fl}$ mice. Statistical significance was determined using a Mann-Whitney's U-test. *$P<0.01$.
doi:10.1371/journal.pone.0011275.g001

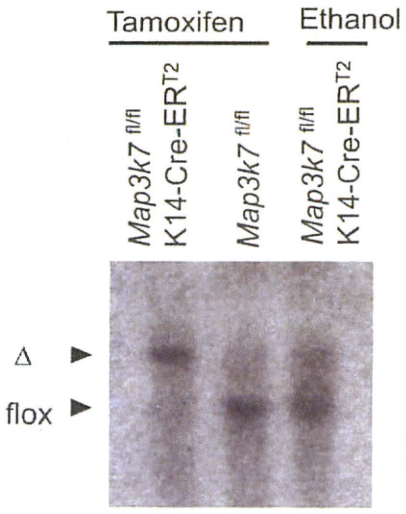

Figure 2. Southern blot analysis. Genomic DNA prepared from the ear skin of mice treated with tamoxifen solution (15 μL/ear) or ethanol for 5 consecutive days was digested with *Xba*I and *Eco*RI. Southern blot analysis for the deletion of the floxed *Tak1* allele was performed as described previously [1]. Cre expression resulted in excision of the floxed allele (*flox*) and generated the deleted allele (Δ) of *Map3k7*.
doi:10.1371/journal.pone.0011275.g002

Although, the skin sample for Southern blot analysis contained non-keratinocyte cells, such as Langerhans cells, melanocytes, or fibroblasts, the band of tamoxifen-treated *Map3k7*$^{fl/fl}$K14-Cre-ER^{T2} mice was a single-recombined band. Since, the majority of this skin sample consists of keratinocytes, flox band of non-keratinocyte cells may not be apparent in this blot. Ethanol-treated *Map3k7*$^{fl/fl}$K14-Cre-ER^{T2} mice also show a minor recombination band, presumably due to slightly leaky Cre- ER^{T2} activity.

Keratinocyte-specific TAK1 deletion results in hair loss in adolescent mice

In the first experiment, tamoxifen was simply applied to the dorsal skin of 8 weeks old mice for 5 consecutive days. Two weeks after the application, the tamoxifen-treated *Map3k7*$^{fl/fl}$K14-Cre-ER^{T2} mice started to lose their hair shafts, and this process continued for more than 4 weeks (Fig. 3). This phenotype suggested the involvement of TAK1 in hair follicle cycling.

Keratinocyte-specific TAK1 deletion delays hair cycle progression in adolescent mice

To further dissect the role of TAK1 in hair follicle cycling, synchronized, active hair growth (anagen) was induced in resting (telogen) hair follicles by wax depilation [26]. This was followed by topical tamoxifen application to the dorsal skin, to delete TAK1 (Fig. 4A). At 2 weeks after synchronized anagen induction, hair shaft formation was noted in the control mice, as a macroscopic indicator of well-advanced anagen development, while hair shaft growth was not seen in the tamoxifen-treated *Map3k7*$^{fl/fl}$K14-Cre-ER^{T2} mice (Fig. 4B). Histological analysis revealed that anagen progression was severely delayed in TAK1-deleted mice at 1–3 weeks (Fig. 4C).

Quantitative hair cycle histomorphometry and hair cycle score calculation (Fig. 5) confirmed that depilation-induced anagen progression was severely delayed in TAK1-deleted mice at 1–3 weeks, while anagen development progressed as expected in TAK1-competent mice. Taken together, these data suggest that

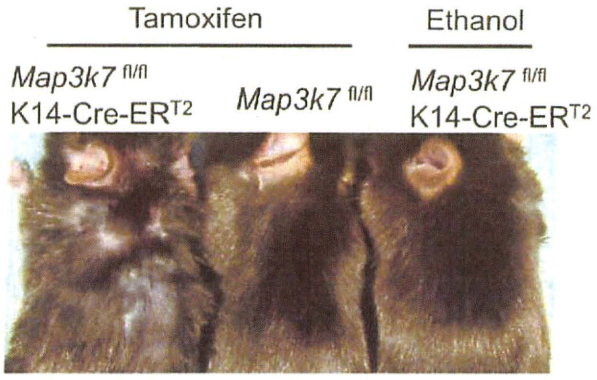

Figure 3. Keratinocyte-specific TAK1 deletion results in hair loss in adolescent mice. Tamoxifen was topically applied to the dorsal skin of the *Map3k7*$^{fl/fl}$K14-Cre-ER^{T2} mice for 5 consecutive days to delete TAK1. The clinical appearance of the mice 4 weeks after the application is shown. As controls, *Map3k7*$^{fl/fl}$ mice or *Map3k7*$^{fl/fl}$K14-Cre-ER^{T2} mice were treated with tamoxifen or ethanol, respectively.
doi:10.1371/journal.pone.0011275.g003

TAK1 is an important regulator of early anagen development in telogen hair follicles, although TAK1 does not appear to be indispensable for anagen induction.

Although leaky Cre- ER^{T2} activity was noted in ethanol-treated *Map3k7*$^{fl/fl}$K14-Cre-ER^{T2} mice (Fig. 2), there was no significant difference between ethanol-treated *Map3k7*$^{fl/fl}$K14-Cre-ER^{T2} mice and tamoxifen-treated *Map3k7*$^{fl/fl}$ mice. Therefore, leaky activity of Cre- ER^{T2} seems to have a minimum effect in this experiment.

Keratinocyte-specific TAK1 deletion causes a transition from anagen to dystrophic catagen in adolescent mice

In the third experimental setup, TAK1 was deleted only 1 week after anagen induction (Fig. 6A). At 2 weeks after depilation, hair regrowth was reduced in the tamoxifen-treated *Map3k7*$^{fl/fl}$K14-Cre-ER^{T2} mice (Fig. 6B), compared with controls. Histological analysis revealed that almost all of the hair follicles in tamoxifen-treated *Map3k7*$^{fl/fl}$K14-Cre-ER^{T2} mice had prematurely entered the apoptosis-driven regression stage of hair follicle cycle (i.e., catagen; Fig. 6C).

Interestingly, however, this accelerated catagen development was associated with striking pigmentary signs of hair follicle damage (dystrophy): many large, ectopically located melanin clumps, often larger than keratinocyte nuclei, were found not only in their normal location (i.e., the precortical hair matrix), but also eccentrically in the hair bulb periphery and in the epithelial strand of the involuting catagen hair follicles (Fig. 6D). Thus, TAK1 deletion induced "dystrophic catagen," an indicator of major hair follicle damage [28]. Quantitative analyses (Fig. 6E) confirmed that most of the hair follicles in tamoxifen-treated *Map3k7*$^{fl/fl}$K14-Cre-ER^{T2} mice were in late dystrophic catagen, while those of controls were in anagen. These data suggest that TAK1 is essential for maintaining a functional anagen phase.

Discussion

Here, we show by mouse genomics and targeted deletion experiments that TAK1, a member of the NF-κB pathway that has chiefly been recognized as a mediator of innate and adaptive immunity [1,2,4,5,6,30], is also a key component of the molecular machinery that controls murine hair growth. Consistent with our previous discovery that TAK1 regulates keratinocyte growth,

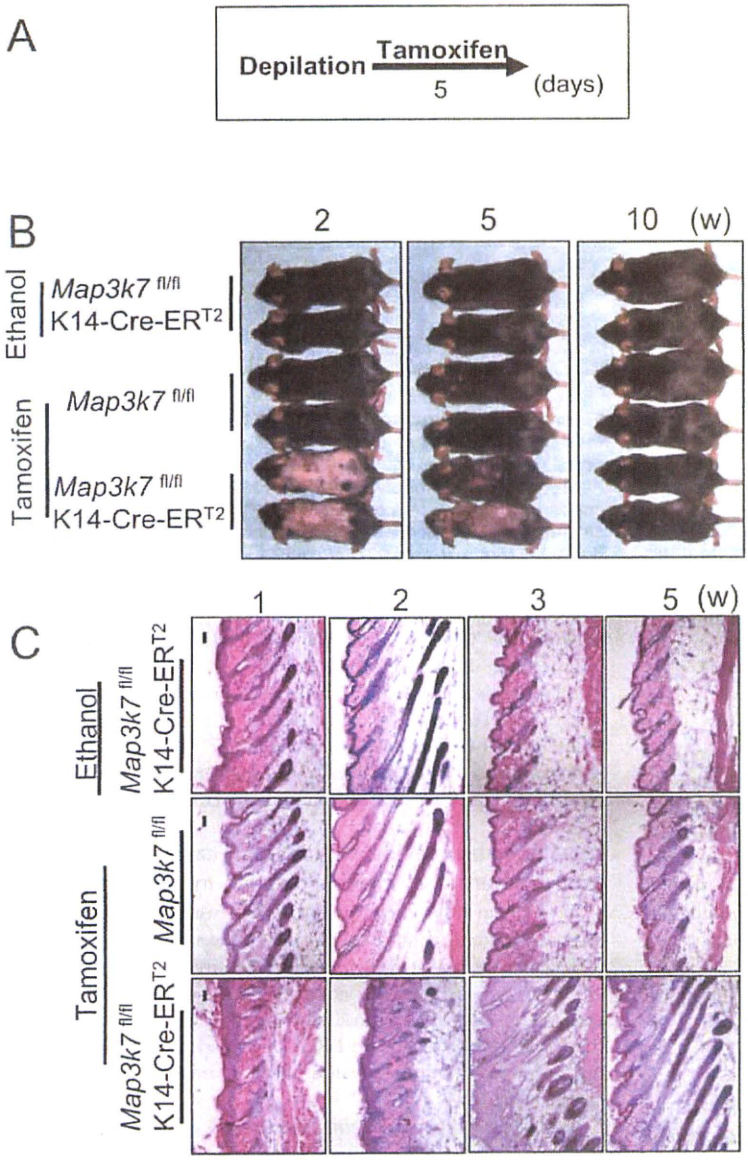

Figure 4. Keratinocyte-specific TAK1 deletion delays hair cycle progression in adolescent mice. (A) Schedule of tamoxifen application. The hair cycle was synchronized to anagen phase by wax depilation, and tamoxifen was topically applied to the dorsal skin of *Map3k7*$^{fl/fl}$K14-Cre-ER^{T2}mice to delete TAK1. As controls, *Map3k7*$^{fl/fl}$ mice or *Map3k7*$^{fl/fl}$K14-Cre-ER^{T2} mice were treated with tamoxifen or ethanol, respectively. (B) Clinical appearance at the indicated time point after the depilation. At 2 weeks, hair shaft formation was noted in the control mice, while hair shaft growth was not seen in the tamoxifen-treated *Map3k7*$^{fl/fl}$K14-Cre-ER^{T2} mice. (C) Histological analysis at the indicated time point after the depilation. Anagen progression was severely delayed in TAK1-deleted mice at 1–3 weeks. Scale bar, 100 μm.
doi:10.1371/journal.pone.0011275.g004

differentiation, and apoptosis [12], we now show that the selective deletion of TAK1 in keratinocytes retards hair follicle induction, morphogenesis, and anagen development, and is required for the maintenance of normal anagen. This newly identified role of TAK1 in hair follicle development and cycling implicates TAK1 as a novel player in complex organ remodeling events and epithelial-mesenchymal interactions, which can be modeled by murine hair follicles [11].

The TAK1-NF-κB pathway regulates not only immune responses [1,30], but also epithelial function [12]. Because the NF-κB pathway controls pro-inflammatory responses, deletion of this pathway was expected to suppress epithelial inflammation. Unexpectedly, however, deletion of TAK1, IKK-β, or IKK-γ was found to result in severe skin inflammation (including abscess formation) [12,31,32,33]. Similarly, a lack of NF-κB signaling produced by the conditional ablation of IKKγ or IKKα and IKKβ in the intestinal epithelium caused severe chronic intestinal inflammation in mice [34]. This suggests that a continuous, basal level of NF-κB activation may be required to maintain epithelial integrity and homeostasis and to suppress excessive skin inflammation. In the current study, we add to the established role of TAK1 in murine skin the novel function of hair growth control.

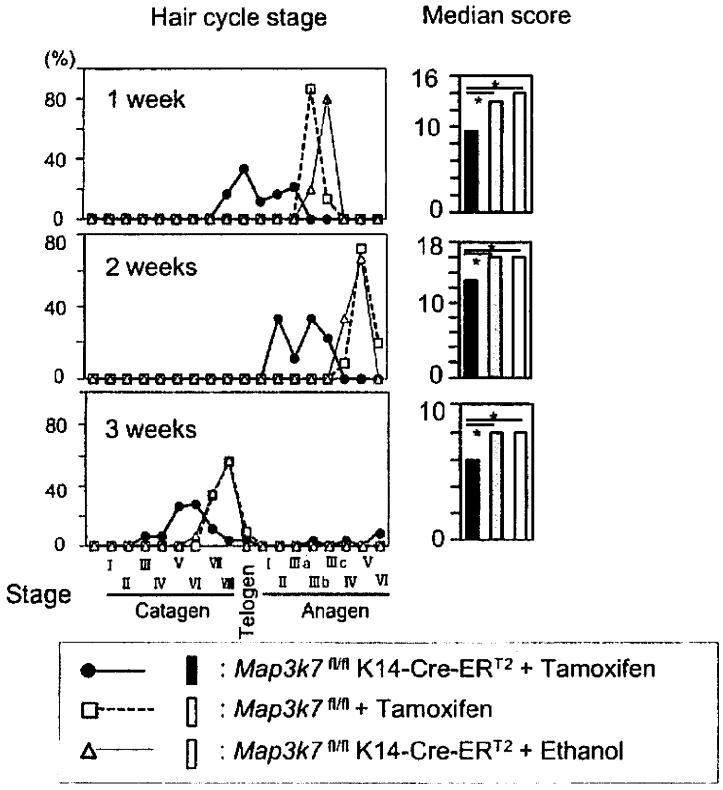

Figure 5. Quantitative hair cycle analysis. Hair cycle stage of each hair follicle in each mouse group in Fig. 4 was evaluated according to our previous report [27]. Then, the rate (%) of a certain hair cycle stage in the total hair follicles (left panel) and the median score in each mouse group (right panel) were determined. The score of tamoxifen-treated *Map3k7*$^{fl/fl}$K14-Cre-ER^{T2} mice was compared with tamoxifen-treated *Map3k7*$^{fl/fl}$ mice or ethanol-treated *Map3k7*$^{fl/fl}$K14-Cre-ER^{T2} mice. Statistical significance was determined using a Mann-Whitney's U-test. *$P<0.01$.
doi:10.1371/journal.pone.0011275.g005

Since TAK1 regulates keratinocyte function [12], there is a possibility that hair follicle defects in TAK1-deficient mice might be attributed to such abnormal capacities of keratinocytes rather than reflecting the specific function of TAK1 in hair follicle regulation. However, clinical skin pheno types and histological abnormalities were not apparent at birth and started to appear at P2 in *Map3k7*$^{fl/fl}$K5-Cre mice [12]. On the other hand, E15.5 is the time point when the defect of hair follicle development became apparent (Fig. 1). Therefore, the defect of hair follicle development is primarily due to the defect of TAK1 signaling during embryogenesis, rather than the functional defect of keratinocytes.

Recently, TAK1 binding protein (TAB) 2 has been identified as a binding partner of EdaR-associated death domain protein (EDARADD) using a yeast two-hybrid screening [35]. In 293 cells, endogenous and overexpressed TAB2, TRAF6 and TAK1 were co-immunoprecipitated with EDARADD [35]. Furthermore, dominant negative forms of TAB2, TRAF6 and TAK1 blocked the NF-κB activation induced by EDARADD in 293 cells[35]. Therefore, it is suggested that TAK1 is involved in hair follicle development. However, the actual role of TAK1 in hair follicle has not been studied before.

The coats of mice contain four major hair follicle subpopulations: guard hairs, awl and auchene hairs, and zigzag hairs. Formation of each kind of hair follicle starts at E14, E16, and E18-P3, respectively and the regulatory mechanisms of hair follicle development are slightly different among them [7,36]. Epidermal NF-κB activity is first observed in the placodes of primary guard hairs at E14.5 [36]. In the absence of NF-κB activity, downstream events, such as maintenance of Wnt signaling and an increase of Wnt10a, Wnt10b, and Dkk4 expression, are impaired [8] and further placode down-growth does not occur in primary guard hair follicles [36]. In *Map3k7*$^{fl/fl}$K5-Cre mice, the number of hair germs was significantly reduced at E15.5, indicating that the development of primary guard hair follicles was greatly impaired. Impaired development of primary guard hair follicles at E15.5 can be explained by the absence of NF-κB activity, due to TAK1 deficiency, consistent with a model in which TAK1 is involved in the EdaA1/EdaR/NF-κB pathway [35] (see Fig. 7). The appearance of a few primary hair placodes might be explained by incomplete TAK1 deletion at E15.5.

In contrast, EdaR/NF-κB activity is dispensable for the induction of awl/auchene hair follicles, as seen in *tabby*, *downless*, and $c^{h/Bz-4}$ mice, even though EdaR/NF-κB-defective, awl/auchene hair follicles subsequently produce abnormal awl-like hair shafts [36,37]. EdaR/NF-κB independent Wnt/β-catenin signaling is required for this process [8]. Thus, the placodes that became visible in *Map3k7*$^{fl/fl}$K5-Cre mice at E16.5 are likely to represent placodes of awl/auchene hair follicles. In a recent study, analyses of Eda and EdaR homologue Troy double-mutant mice revealed that, in addition to primary guard hair follicles, awl/auchene hair follicles were defective in these mice [38]. This study suggested that EdaR and Troy redundantly activate an NF-κB independent pathway, via TRAF6, to develop awl/auchene hair follicle placodes. Therefore, it is conceivable that placode development

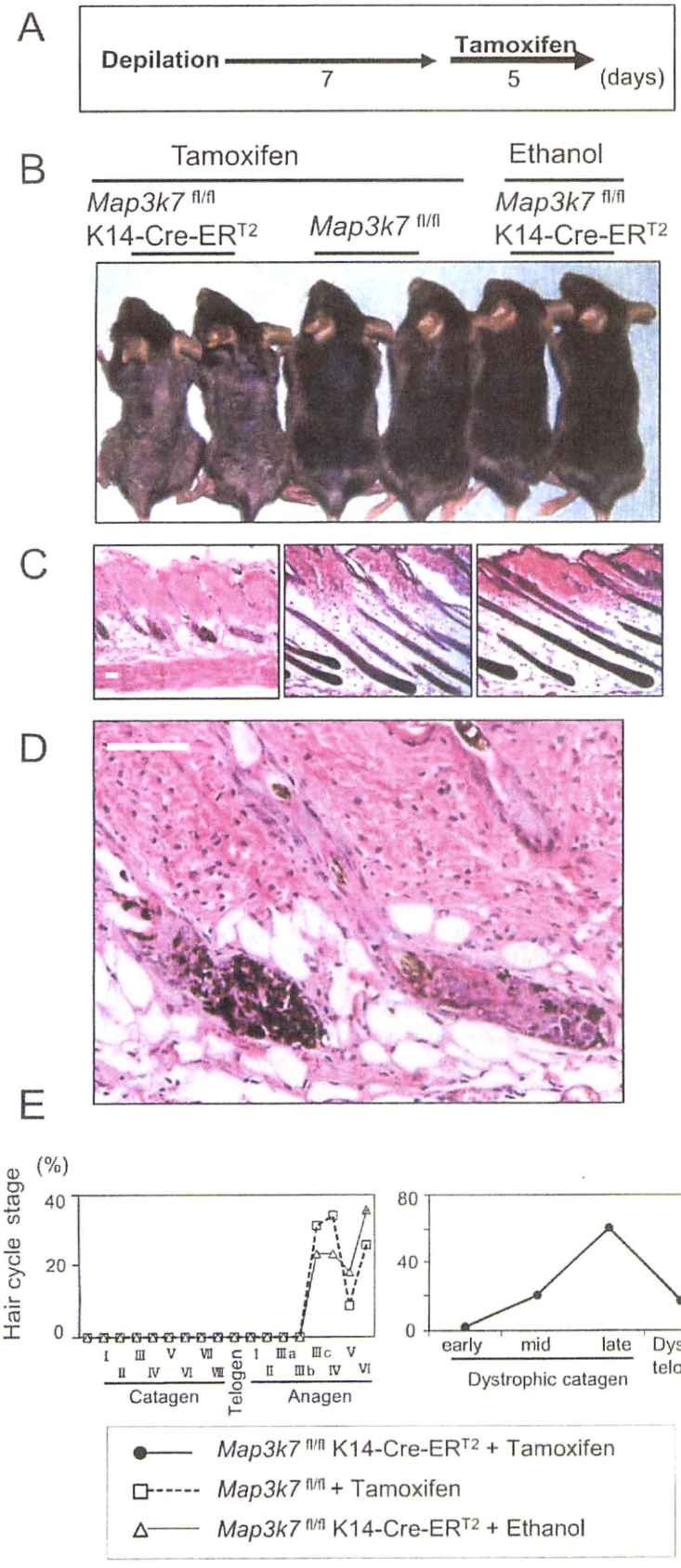
A
Depilation
7
Tamoxifen
5
(days)
B
Tamoxifen
Ethanol
Map3k7 fl/fl
K14-Cre-ERT2
Map3k7 fl/fl
Map3k7 fl/fl
K14-Cre-ERT2
C
D
E
(%)
Hair cycle stage
40
20
0
I III V VII
II IV VI VIII
Catagen
Telogen
I IIIa IIIc V
II IIIb IV VI
Anagen
80
40
0
early
mid
late
Dystrophic telogen
Dystrophic catagen
Map3k7 fl/fl K14-Cre-ERT2 + Tamoxifen
Map3k7 fl/fl + Tamoxifen
Map3k7 fl/fl K14-Cre-ERT2 + Ethanol

Figure 6. Keratinocyte-specific TAK1 deletion causes a transition from anagen to dystrophic catagen in adolescent mice. (A) Schedule of tamoxifen application. The hair cycle was synchronized to anagen phase by wax depilation. At 7 days after depilation, tamoxifen was applied for 5 days. (B) Clinical appearance of the mice 2 weeks after depilation. (C) Histological analysis of the mice 2 weeks after depilation. (D) Higher magnification of the tamoxifen-treated *Map3k7*$^{fl/fl}$K14-Cre-ER^{T2} mice in (C). Scale bar, 100 μm. (E) Dystrophic catagen was defined according to a previous report [28]. Then, the rate (%) of a certain hair follicle stage per total hair follicles was calculated. Quantitative analyses confirmed that most of the hair follicles in tamoxifen-treated *Map3k7*$^{fl/fl}$K14-Cre-ER^{T2} mice were in late dystrophic catagen, while those of controls were in anagen.
doi:10.1371/journal.pone.0011275.g006

in *Map3k7*$^{fl/fl}$K5-Cre mice is controlled by this NF-κB- (and TAK1)-independent pathway (Fig. 7).

Besides NF-κB signaling, recent studies indicate the implication of TAK1 in multiple signaling pathways such as MAP kinases and AP1 signaling [1,39], supporting the alternative possibility that, in addition to the NF-κB signaling pathway, multiple signaling pathways may be also involved in hair follicle regulation downstream to TAK1. Although some TNF receptor family activate JNK pathway in addition to NF-κB, Edar shows only weak activation of JNK/AP-1 pathway [14,20]. In contrast to Edar, Troy [40] leads to a strong activation of JNK pathway, but weak activation of NF-κB [20,40]. Therefore, it is possible Troy/TAK1/JNK/AP-1 pathway is involved in hair morphogenesis. However, this point should be further clarified.

An interesting difference was observed between *Map3k7*$^{fl/fl}$K5-Cre mice and *tabby*, *downless*, and $c^{IκBαΔN}$ mice. While *tabby*, *downless*, and $c^{IκBαΔN}$ mice produced abnormal awl-like hair shafts, *Map3k7*$^{fl/fl}$K5-Cre mice exhibited a prolonged morphogenesis period and did not develop hair shafts, even after skin transplantation onto normal control mice (unpublished, preliminary findings). This suggests that TAK1 deletion also affects the morphogenesis of the secondary hair follicles.

Although numerous molecular players have been identified as powerful regulators of hair follicle cycling, the exact molecular machinery that drives the elusive "hair cycle clock" remains unclear [29,41,42,43]. For example, IGF-1, HGF, glial-derived neurotrophic factor, and VEGF are known to prolong the duration of anagen, while fibroblast growth factor 5, TGFβ1 and TGFβ2, IL-1β, NT-3, estrogen receptor-mediated signaling, and IFN-γ are all known to induce the anagen-catagen transition [29,41,43,44,45]. The expression of regulatory molecules is controlled by upstream signals, such as those provided by the NF-κB, Wnt/β-catenin, bone morphogenetic protein (BMP), and Shh-Gli pathways [29,41,42]. On the basis of our findings, TAK1 should now be considered a part of the molecular machinery of the anagen induction.

In the present study, we have shown that TAK1 deletion severely delays the telogen-anagen transition, although it is not completely suppressed, while deletion of TAK1 in anagen follicles prematurely induces catagen and damages normal hair follicle function. Thus, TAK1 activity is important, but not essential, for anagen initiation and progression, yet is essential for the maintenance of mature anagen follicles, with loss of TAK1 activity resulting in catagen induction. The next challenge is to dissect the upstream and downstream signals of TAK1. Because NF-κB is thought to be a downstream signal of TAK1 in hair morphogenesis, and because strong NF-κB activity is detected in the anagen matrix of pelage follicles of adult mice [37], NF-κB is a major candidate downstream signal of TAK1 in anagen induction. Conversely, EdaR is a plausible candidate upstream signal of TAK1 because EdaA1 and EdaR have already been shown to be involved in hair follicle cycling [9,21,22].

After chemical, biological, or physical damage, hair follicles develop abnormalities that are collectively called hair follicle dystrophy [28]. Low follicular damage induces the "dystrophic anagen" response. Severe follicular damage induces the "dystrophic catagen" response, characterized by an immediate anagen termination. In Fig. 6, the hair follicle stage was defined as "dystrophic catagen". The development of "dystrophic catagen" indicates TAK1-deletion-induced follicular damage is comparatively higher and similar to those of high dose cyclophosphamide-induced alopecia. These suggest that TAK1-deletion-induced dystrophic catagen could be a model of chemotherapy-induced alopecia.

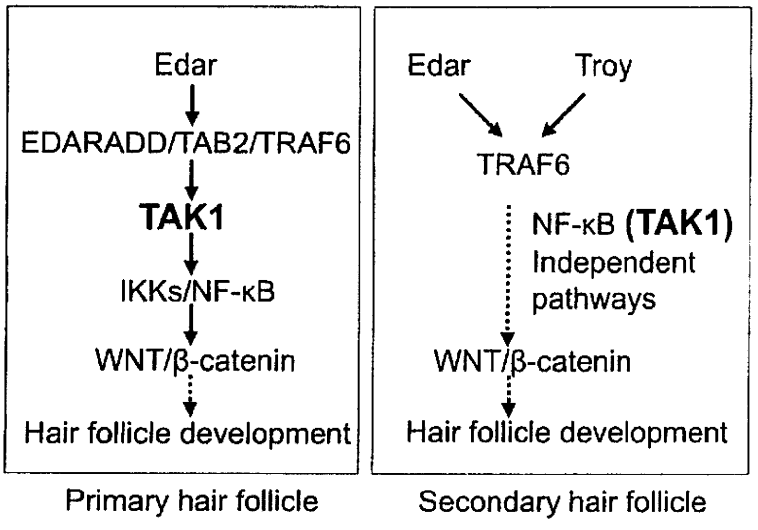

Figure 7. Model for the signaling pathways involved in hair follicle development. In the development of primary hair placodes, TAK1 is involved in the Edar/NF-κB pathway. In secondary hair placodes, NF-κB (TAK1)-independent pathways regulate hair placode development.
doi:10.1371/journal.pone.0011275.g007

The evidence reported here, that TAK1, a critical mediator of inflammation [1,30], is also involved in hair morphogenesis and anagen induction.

Acknowledgments

We thank Manabu Ohyama (Keio University, Tokyo, Japan), Teruko Tsuda, and Eriko Tan (Ehime University) for providing significant technical assistance.

Author Contributions

Conceived and designed the experiments: KS KH. Performed the experiments: KS KK KS SS YH XD. Analyzed the data: KS SH YS YTT RP JK. Contributed reagents/materials/analysis tools: DM PC SA. Wrote the paper: KS RP.

References

1. Sato S, Sanjo H, Takeda K, Ninomiya-Tsuji J, Yamamoto M, et al. (2005) Essential function for the kinase TAK1 in innate and adaptive immune responses. Nat Immunol 6: 1087–1095.
2. Shim JH, Xiao C, Paschal AE, Bailey ST, Rao P, et al. (2005) TAK1, but not TAB1 or TAB2, plays an essential role in multiple signaling pathways in vivo. Genes Dev 19: 2668–2681.
3. Yamaguchi K, Shirakabe K, Shibuya H, Irie K, Oishi I, et al. (1995) Identification of a member of the MAPKKK family as a potential mediator of TGF-beta signal transduction. Science 270: 2008–2011.
4. Takaesu G, Kishida S, Hiyama A, Yamaguchi K, Shibuya H, et al. (2000) TAB2, a novel adaptor protein, mediates activation of TAK1 MAPKKK by linking TAK1 to TRAF6 in the IL-1 signal transduction pathway. Mol Cell 5: 649–658.
5. Takaesu G, Surabhi RM, Park KJ, Ninomiya-Tsuji J, Matsumoto K, et al. (2003) TAK1 is critical for IkappaB kinase-mediated activation of the NF-kappaB pathway. J Mol Biol 326: 105–115.
6. Ishitani T, Takaesu G, Ninomiya-Tsuji J, Shibuya H, Gaynor RB, et al. (2003) Role of the TAB2-related protein TAB3 in IL-1 and TNF signaling. Embo J 22: 6277–6288.
7. Schmidt-Ullrich R, Paus R (2005) Molecular principles of hair follicle induction and morphogenesis. Bioessays 27: 247–261.
8. Zhang Y, Tomann P, Andl T, Gallant NM, Huelsken J, et al. (2009) Reciprocal requirements for EDA/EDAR/NF-kappaB and Wnt/beta-catenin signaling pathways in hair follicle induction. Dev Cell 17: 49–61.
9. Tong X, Coulombe PA (2006) Keratin 17 modulates hair follicle cycling in a TNFalpha-dependent fashion. Genes Dev 20: 1353–1364.
10. Courtney JM, Blackburn J, Sharpe PT (2005) The Ectodysplasin and NFkappaB signalling pathways in odontogenesis. Arch Oral Biol 50: 159–163.
11. Schneider MR, Schmidt-Ullrich R, Paus R (2009) The hair follicle as a dynamic miniorgan. Curr Biol 19: R132–142.
12. Sayama K, Hanakawa Y, Nagai H, Shirakata Y, Dai X, et al. (2006) Transforming growth factor-beta-activated kinase 1 is essential for differentiation and the prevention of apoptosis in epidermis. J Biol Chem 281: 22015–22020.
13. Paus R, Muller-Rover S, Van Der Veen C, Maurer M, Eichmuller S, et al. (1999) A comprehensive guide for the recognition and classification of distinct stages of hair follicle morphogenesis. J Invest Dermatol 113: 523–532.
14. Mikkola ML, Thesleff I (2003) Ectodysplasin signaling in development. Cytokine Growth Factor Rev 14: 211–224.
15. Kere J, Srivastava AK, Montonen O, Zonana J, Thomas N, et al. (1996) X-linked anhidrotic (hypohidrotic) ectodermal dysplasia is caused by mutation in a novel transmembrane protein. Nat Genet 13: 409–416.
16. Ferguson BM, Brockdorff N, Formstone E, Ngyuen T, Kronmiller JE, et al. (1997) Cloning of Tabby, the murine homolog of the human EDA gene: evidence for a membrane-associated protein with a short collagenous domain. Hum Mol Genet 6: 1589–1594.
17. Srivastava AK, Pispa J, Hartung AJ, Du Y, Ezer S, et al. (1997) The Tabby phenotype is caused by mutation in a mouse homologue of the EDA gene that reveals novel mouse and human exons and encodes a protein (ectodysplasin-A) with collagenous domains. Proc Natl Acad Sci U S A 94: 13069–13074.
18. Yan M, Wang LC, Hymowitz SG, Schilbach S, Lee J, et al. (2000) Two-amino acid molecular switch in an epithelial morphogen that regulates binding to two distinct receptors. Science 290: 523–527.
19. Headon DJ, Emmal SA, Ferguson BM, Tucker AS, Justice MJ, et al. (2001) Gene defect in ectodermal dysplasia implicates a death domain adapter in development. Nature 414: 913–916.
20. Kumar A, Eby MT, Sinha S, Jasmin A, Chaudhary PM (2001) The ectodermal dysplasia receptor activates the nuclear factor-kappaB, JNK, and cell death pathways and binds to ectodysplasin A. J Biol Chem 276: 2668–2677.
21. Fessing MY, Sharova TY, Sharov AA, Atoyan R, Botchkarev VA (2006) Involvement of the Edar signaling in the control of hair follicle involution (catagen). Am J Pathol 169: 2075–2084.
22. Mustonen T, Pispa J, Mikkola ML, Pummila M, Kangas AT, et al. (2003) Stimulation of ectodermal organ development by Ectodysplasin-A1. Dev Biol 259: 123–136.
23. Tarutani M, Itami S, Okabe M, Ikawa M, Tezuka T, et al. (1997) Tissue-specific knockout of the mouse Pig-a gene reveals important roles for GPI-anchored proteins in skin development. Proc Natl Acad Sci U S A 94: 7400–7405.
24. Li M, Indra AK, Warot X, Brocard J, Messaddeq N, et al. (2000) Skin abnormalities generated by temporally controlled RXRalpha mutations in mouse epidermis. Nature 407: 633–636.
25. Indra AK, Warot X, Brocard J, Bornert JM, Xiao JH, et al. (1999) Temporally-controlled site-specific mutagenesis in the basal layer of the epidermis: comparison of the recombinase activity of the tamoxifen-inducible Cre-ER(T) and Cre-ER(T2) recombinases. Nucleic Acids Res 27: 4324–4327.
26. Paus R, Slominski AS, Czarnetzki BM (1990) Telogen skin contains an inhibitor of hair growth. Br J Dermatol 122: 777–784.
27. Muller-Rover S, Handjiski B, van der Veen C, Eichmuller S, Foitzik K, et al. (2001) A comprehensive guide for the accurate classification of murine hair follicles in distinct hair cycle stages. J Invest Dermatol 117: 3–15.
28. Heudrix S, Handjiski B, Peters EM, Paus R (2005) A guide to assessing damage response pathways of the hair follicle: lessons from cyclophosphamide-induced alopecia in mice. J Invest Dermatol 125: 42–51.
29. Paus R, Foitzik K (2004) In search of the "hair cycle clock": a guided tour. Differentiation 72: 489–511.
30. Sato S, Sanjo H, Tsujimura T, Ninomiya-Tsuji J, Yamamoto M, et al. (2006) TAK1 is indispensable for development of T cells and prevention of colitis by the generation of regulatory T cells. Int Immunol 18: 1405–1411.
31. Sraons A, Pasparakis M, Markur D, Knaup R, Pofahl R, et al. (2006) Localized inflammatory skin disease following inducible ablation of I kappa B kinase 2 in murine epidermis. J Invest Dermatol 126: 614–620.
32. Makris C, Godfrey VL, Krahn-Senftleben G, Takahashi T, Roberts JL, et al. (2000) Female mice heterozygous for IKK gamma/NEMO deficiencies develop a dermatopathy similar to the human X-linked disorder incontinentia pigmenti. Mol Cell 5: 969–979.
33. Schmidt-Supprian M, Bloch W, Courtois G, Addicks K, Israel A, et al. (2000) NEMO/IKK gamma-deficient mice model incontinentia pigmenti. Mol Cell 5: 981–992.
34. Nenci A, Becker C, Wullaert A, Gareus R, van Loo G, et al. (2007) Epithelial NEMO links innate immunity to chronic intestinal inflammation. Nature 446: 557–561.
35. Morlon A, Munnich A, Smahi A (2005) TAB2, TRAF6 and TAK1 are involved in NF-kappaB activation induced by the TNF-receptor, Edar and its adaptator Edaradd. Hum Mol Genet 14: 3751–3757.
36. Schmidt-Ullrich R, Tobin DJ, Lenhard D, Schneider P, Paus R, et al. (2006) NF-kappaB transmits Eda A1/EdaR signalling to activate Shh and cyclin D1 expression, and controls post-initiation hair placode down growth. Development 133: 1045–1057.
37. Schmidt-Ullrich R, Aebischer T, Hulsken J, Birchmeier W, Klemm U, et al. (2001) Requirement of NF-kappaB/Rel for the development of hair follicles and other epidermal appendices. Development 128: 3843–3853.
38. Pispa J, Pummila M, Barker PA, Thesleff I, Mikkola ML (2008) Edar and Troy signalling pathways act redundantly to regulate initiation of hair follicle development. Hum Mol Genet 17: 3380–3391.
39. Sakurai H, Nishi A, Sato N, Mizukami J, Miyoshi H, et al. (2002) TAK1-TAB1 fusion protein: a novel constitutively active mitogen-activated protein kinase kinase kinase that stimulates AP-1 and NF-kappaB signaling pathways. Biochem Biophys Res Commun 297: 1277–1281.
40. Kojima T, Morikawa Y, Copeland NG, Gilbert DJ, Jenkins NA, et al. (2000) TROY, a newly identified member of the tumor necrosis factor receptor superfamily, exhibits a homology with Edar and is expressed in embryonic skin and hair follicles. J Biol Chem 275: 20742–20747.
41. Sveen KS, Paus R (2001) Controls of hair follicle cycling. Physiol Rev 81: 449–494.
42. Alonso L, Fuchs E (2006) The hair cycle. J Cell Sci 119: 391–393.
43. Ohnemus U, Uenalan M, Inzunza J, Gustafsson JA, Paus R (2006) The hair follicle as an estrogen target and source. Endocr Rev 27: 677–706.
44. Mecklenburg L, Tobin DJ, Muller-Rover S, Handjiski B, Wendt G, et al. (2000) Active hair growth (anagen) is associated with angiogenesis. J Invest Dermatol 114: 909–916.
45. Lindner G, Menrad A, Gherardi E, Merlino G, Welker P, et al. (2000) Involvement of hepatocyte growth factor/scatter factor and met receptor signaling in hair follicle morphogenesis and cycling. Faseb J 14: 319–332.

THE JOURNAL OF BIOLOGICAL CHEMISTRY VOL. 285, NO. 39, pp. 30042–30049, September 24, 2010

E2 Polyubiquitin-conjugating Enzyme Ubc13 in Keratinocytes Is Essential for Epidermal Integrity*

Received for publication, January 21, 2010, and in revised form, July 5, 2010 Published, JBC Papers in Press, July 27, 2010, DOI 10.1074/jbc.M110.106484

Koji Sayama[‡1,2], **Masahiro Yamamoto**[§1], **Yuji Shirakata**[‡], **Yasushi Hanakawa**[‡], **Satoshi Hirakawa**[‡], **Xiuju Dai**[‡], **Mikiko Tohyama**[‡], **Sho Tokumaru**[‡], **Myoung-Sook Shin**[¶], **Hiroaki Sakurai**[¶], **Shizuo Akira**[§], **and Koji Hashimoto**[‡]

From the [‡]*Department of Dermatology, Ehime University Graduate School of Medicine, Ehime 791-0295, Japan, the* [§]*Research Institute for Microbial Disease, Osaka University, Suita 565-0871, Japan, and the* [¶]*Division of Pathogenic Biochemistry, Institute of Natural Medicine, University of Toyama, Toyama 930-0194, Japan*

The E2 polyubiquitin-conjugating enzyme Ubc13 is a mediator of innate immune reactions. Ubc13 mediates the conjugation of keratin (K)63-linked polyubiquitin chains onto TNF receptor-associated factor 6 and IKKγ during NF-κB activation. In contrast to K48-linked polyubiquitin chains, K63-linked polyubiquitin chains function in nonproteasomal biological processes. Although Ubc13 has been shown to be critical for Toll-like receptor (TLR) and IL-1 receptor signaling, the function of Ubc13 in the epidermis has not been studied. We generated keratinocyte-specific Ubc13-deficient mice (*$Ubc13^{flox/flox}$*K5-Cre). At birth, the skin of the *$Ubc13^{flox/flox}$*K5-Cre mice was abnormally shiny and smooth; in addition, the mice did not grow and died by postnatal day 2. Histological analysis showed atrophy of the epidermis with keratinocyte apoptosis. Immunohistochemical analyses revealed reduced proliferation, abnormal differentiation, and apoptosis of keratinocytes in the *$Ubc13^{flox/flox}$*K5-Cre mouse epidermis. In culture, *$Ubc13^{flox/flox}$*K5-Cre keratinocyte growth was impaired, and spontaneous cell death occurred. Moreover, the deletion of Ubc13 from cultured *$Ubc13^{flox/flox}$* keratinocytes by means of an adenoviral vector carrying Cre recombinase also resulted in spontaneous cell death. Therefore, Ubc13 is essential for keratinocyte growth, differentiation, and survival. Analyses of intracellular signaling revealed that the IL-1 and TNF-induced activation of JNK, p38, and NF-κB pathways was impaired in *$Ubc13^{flox/flox}$*K5-Cre keratinocytes. In conclusion, Ubc13 appears to be essential for epidermal integrity in mice.

The NF-κB, JNK, and p38 intracellular signaling cascades mediate innate immune or pro-inflammatory responses such as TLR, IL-1 receptor, and TNF receptor signaling (1, 2). Upon stimulation, TNF receptor-associated factor 6 is polyubiquitinated, which induces it to phosphorylate TGF-β-activated kinase 1 (TAK1)[3] (3, 4). The polyubiquitin chains on TNF receptor-associated factor 6 are generated by the E2 ubiquitin-conjugating enzyme Ubc13 (3, 5). Ubc13 conjugates keratin (K)63-linked polyubiquitin chains to TNF receptor-associated factor 6 and IKK-γ. In contrast to K48-linked polyubiquitin chains, K63-linked polyubiquitin chains function in nonproteasomal biological processes, such as stress responses, rather than protein destruction. However, the role of these signaling molecules varies by cell type and stimulus.

Epidermal keratinocytes proliferate at the basal cell layer and then differentiate to form the multilayered epidermis, which serves as a physical barrier against the external environment. The proliferation and differentiation of keratinocytes are regulated by intracellular signaling pathways, including those mediated by NF-κB, MAPK, and PI3K (6–8). In this study, we focused on the NF-κB pathway. Genetic studies have shown that mutations in *NEMO/IKK-γ* cause incontinentia pigmenti or Bloch-Sulzberger syndrome in humans (9). The disruption of *NEMO/IKK-γ* leads to hyperproliferation and increased apoptosis in keratinocytes (10, 11). The functional blockade of NF-κB *in vivo* by the expression of a dominant-negative mutant of NF-κB in mouse epidermis resulted in a hyperplastic epithelium (6). Similarly, a deficiency in the p65 subunit of NF-κB caused hyperplasia of the epidermis (12). In addition to the regulation of differentiation and cell growth, NF-κB protects keratinocytes from apoptosis. The blockade of NF-κB function in the epidermis by the expression of a dominant-negative mutant of IκBα provoked premature spontaneous cell death (13). TAK1 is a critical mediator of NF-κB activation. Previously, we generated keratinocyte-specific TAK1-deficient mice and showed that along with IKKs, TAK1 regulates keratinocyte growth, differentiation, and apoptosis (14).

Because Ubc13 functions in the NF-κB signaling pathway, it might be expected to regulate keratinocyte growth, differentiation, and apoptosis. However, the function of Ubc13 in epidermal keratinocytes has not been studied. To address this issue, we generated keratinocyte-specific Ubc13-deficient mice by breeding *$Ubc13^{flox/flox}$* mice (15) with mice carrying the Cre transgene under the control of the keratin-5 promoter (K5-Cre) (16).

* This work was supported by grants from the Ministries of Education, Culture, Sports, Science, and Technology of Japan; by Health and Labor Sciences Research Grants (Research on Intractable Diseases) from the Ministry of Health, Labor, and Welfare of Japan; and by grants from the Takeda Science Foundation, Mishima Kaiun Memorial Foundation, Mochida Memorial Foundation for Medical and Pharmaceutical Research, Naito Foundation, Kowa Life Science Foundation, and the Yasuda Medical Foundation.

[1] Both authors contributed equally to this work.

[2] To whom correspondence should be addressed: Dept. of Dermatology, Ehime University Graduate School of Medicine, Toon, Ehime 791-0295, Japan. Fax: 81-89-960-5352; E-mail: sayama@m.ehime-u.ac.jp.

[3] The abbreviations used are: TAK1, TGF-β-activated kinase 1; K, keratin; Ax, adenoviral vector; LDH, lactate dehydrogenase; HB-EGF, heparin-binding EGF-like growth factor; TLR, toll-like receptor; TRAIL, TNF-related apoptosis-inducing ligand.

EXPERIMENTAL PROCEDURES

Generation of Keratinocyte-specific Ubc13-deficient Mice Using Gene Targeting with the Cre Transgene—The targeting construct was described previously (15). *Ubc13*$^{flox/flox}$ mice were bred with K5-Cre mice (generous gift from Junji Takeda, Osaka University, Osaka, Japan) (16) to generate K5-Cre/*Ubc13*$^{flox/+}$ mice. Subsequently, the K5-Cre/*Ubc13*$^{flox/+}$ mice were bred with *Ubc13*$^{flox/flox}$ mice to generate K5-Cre/*Ubc13*$^{flox/flox}$ mice. This protocol was approved by the Institutional Review Board of the Ehime University Graduate School of Medicine.

The genotype was confirmed by Southern and Western blotting as described previously (15). Genomic DNA was extracted from the tails of the mice, digested with NcoI and ScaI, electrophoresed, and hybridized with a radiolabeled probe (15). For Western blot analysis, newborn mouse keratinocytes were cultured overnight, and adherent keratinocytes were harvested for analysis.

Histological Analysis—To analyze the expression of the differentiation markers K5, K14, K1, K10, and loricrin, paraffin-embedded sections were deparaffinized, blocked with 10% goat serum, and reacted with primary antibodies overnight at 4 °C. After washing, the antibodies were detected using a peroxidase staining kit (ImmPRESS; Vector Laboratories, Burlingame, CA) and visualized with aminoethyl carbazole. For K15 and Ki67 staining, the deparaffinized sections were boiled in 10 mM citrate buffer, pH 6.0, for 40 min and cooled at room temperature for 20 min for antigen retrieval.

TUNEL—Keratinocyte apoptosis was detected using the TUNEL method as described previously (14) using an *in situ* detection kit (Roche Applied Science).

Antibodies—The following antibodies were used: Covance); Ki67 (MM1; Novo Castra); β-actin (AC-15; Abcam); IKK-γ (sc-8330; Santa Cruz Biotechnology); ubiquitin (P4D1; Santa Cruz Biotechnology); mouse TNF-α (goat; R & D Systems); and Ubc13 (4E11; Zymed Laboratories); cIAP-2 (mouse; R & D Systems); and caspase-3 (rabbit; Cell Signaling Technology). Antibodies specific for the phosphorylation forms of ERK (9101), JNK (9251), and p38 (9211) were purchased from Cell Signaling Technology.

Preparation of the Ax—An Ax encoding Cre-recombinase (Ax-Cre) was prepared as described previously (14). We infected the keratinocytes with the Ax at a multiplicity of infection of 100. Ax carrying LacZ (Ax-LacZ) was used as a control.

Keratinocyte Culture—Primary mouse keratinocytes were isolated from newborn mouse skin and cultured as described previously (14) using CnT-07 medium (CellnTec, Bern, Switzerland).

For the analysis of cell growth, freshly isolated newborn mouse keratinocytes were allowed to adhere to the culture dishes for several hours, and the nonadherent cells were removed by washing. The number of adherent cells was counted using a Coulter Counter (Beckman Coulter); this was denoted day 0. Cell culture continued for 3 days. The number of cells at day 0 was referred to as 100%.

For cytotoxic analysis, freshly isolated newborn mouse keratinocytes were stimulated with mouse TNF-α (Kamiya Biomedical Company; 10 ng/ml) or anti-mouse TNF-α (5 μg/ml). At 48 h, the supernatant was harvested for use in the LDH assay. Next, Ubc13 was deleted in *Ubc13*$^{flox/flox}$ keratinocytes by transfection of Ax-Cre at a multiplicity of infection of 100. Finally, 24 h after transfection, keratinocytes were stimulated with TNF-α or anti-TNF-α for 48 h. For analysis of intracellular signaling, freshly isolated newborn mouse keratinocytes were stimulated soon after adherence to cell culture dishes with IL-1β (PeproTech EC, London, UK; 10 ng/ml), TNF-α (10 ng/ml), or HB-EGF (R & D Systems; 10 ng/ml).

Western Blotting—Keratinocytes were harvested on ice with lysis buffer, and Western blotting was performed as described previously (8) using a FluorolImager (Molecular Dynamics). Phosphorylation of TAK1 was analyzed as described previously (1).

Immunoprecipitation—The cell lysates were precleaned with protein G-Sepharose (Amersham Biosciences) for 2 h and then incubated with protein G-Sepharose containing 1.0 μg of anti-IKK-γ for 12 h with rotating at 4 °C. After washing, the sample was eluted by boiling with sample buffer and then subjected to Western blot analysis using anti-ubiquitin as described previously (15).

LDH Assay—Cell death was quantitated by measuring LDH release using an LDH assay kit (Kyokutokogyo, Tokyo, Japan) according to the manufacturer's instructions. LDH from the living cells was obtained by cell lysis with 0.1% Tween 20. LDH release was expressed as a percentage of the total LDH, which was obtained by summing the LDH released and the LDH of the living cells. The data are expressed as the means ± S.E.

EMSA—Nuclear proteins were isolated, and 5 μg of proteins were applied for EMSA analyses as described previously (17) using a Light Shift Chemiluminescent EMSA kit (Pierce) according to the manufacturer's instructions. Specific NF-κB probe sets (biotin-labeled and unlabeled probes) were obtained from Panomics (Redwood City, CA). Protein-DNA complexes were separated and transferred to Biodyne B nylon membranes (Pierce). In competition experiments, unlabeled probes were added at 200-fold molar excess. The biotin-labeled molecules in the membranes were detected using a Chemiluminescent nucleic acid detection module (Pierce) and exposed to x-ray film.

Real Time PCR—Newborn mouse epidermis was separated from the dermis by heat treatment at 60 °C for 30 s. mRNA was extracted from the epidermis and was subjected to real time PCR analyses as described previously (18). The primers and the probes used for GAPDH, IL-1β, and TNF-α were obtained from Applied Biosystems (Branchburg, NJ). Gene expression levels were quantified using the comparative CT method and were normalized against GAPDH (18). The mean value of *Ubc13*$^{flox/flox}$ mice was referred to as 1.0 unit.

Luciferase Assay—pNFκB-TA-Luc (Clontech) was transfected to the keratinocytes. To normalize the transfection efficiency, pRL-TK (Promega) was included in the assay. The reporter plasmids were introduced into keratinocytes using FuGENE 6 (Roche Applied Science) according to the manufacturer's instructions. After treatment, the same number of cells was harvested with 250 μl of lysis buffer (Promega), and the luciferase activity was measured using the dual luciferase reporter

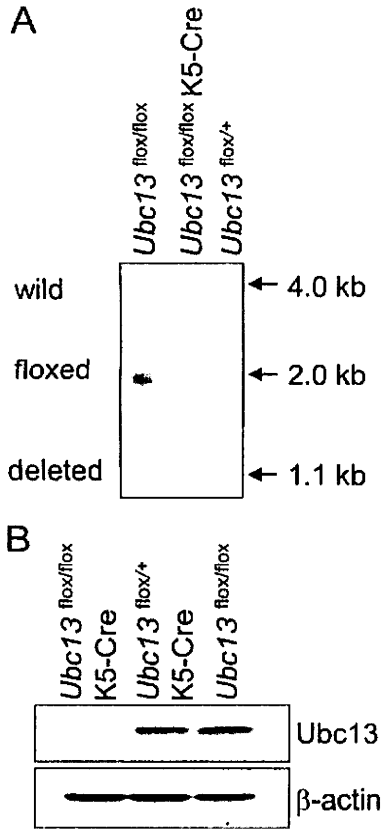

FIGURE 1. **Generation of keratinocyte-specific Ubc13-deficient mice.** Keratinocyte-specific Ubc13-deficient mice were generated by breeding *Ubc13*$^{flox/flox}$ mice (15) with K5-Cre mice (16). Southern (*A*) and Western (*B*) blotting confirmed the genotype. *A*, genomic DNA was extracted from mouse tails, digested with NcoI and ScaI, electrophoresed, and hybridized with a radiolabeled probe (15). *4.0-kb band*, wild-type allele; *2.0-kb band*, floxed allele; *1.1-kb band*, deleted allele. *B*, newborn mouse keratinocytes were cultured overnight, and the adherent keratinocytes were harvested for Western blot analysis. β-Actin was used as an internal standard.

assay system (Promega) with a luminometer (Luminescencer JNR AB-2100; Atto, Japan). The relative luciferase activity was calculated by normalizing to the level of *Renilla* luciferase activity.

Statistical Analysis—Statistical significance was determined using a paired Student's *t* test. A difference of $p < 0.01$ (*) or $p < 0.05$ (**) was considered statistically significant.

RESULTS

Generation of Keratinocyte-specific Ubc13-deficient Mice—Because the germ line deletion of *Ubc13* results in embryonic lethality (15), we generated keratinocyte-specific Ubc13-deficient mice by breeding *Ubc13*$^{flox/flox}$ mice (15) with K5-Cre mice (16). Southern and Western blot analyses showed the efficient deletion of Ubc13 in keratinocytes collected from *Ubc13*$^{flox/flox}$ K5-Cre mice at birth (Fig. 1).

Skin Phenotypes of the Ubc13$^{flox/flox}$*K5-Cre Mice at Birth*—At birth, the skin of the *Ubc13*$^{flox/flox}$ K5-Cre mice was abnormally shiny and smooth (Fig. 2*A*). In addition, the mice did not grow and died by postnatal day 2. In comparison, *Ubc13*$^{flox/+}$ and *Ubc13*$^{+/+}$ mice with or without K5-Cre showed no pathological phenotypes.

Histological analysis revealed atrophy of the epidermis in the *Ubc13*$^{flox/flox}$ K5-Cre mice (Fig. 2*B*), indicating that cell growth is impaired by the deletion of Ubc13. Ki67 staining showed decreased keratinocyte proliferation, whereas H&E staining and TUNEL revealed the presence of a small number of apoptotic cells, in the epidermis of each *Ubc13*$^{flox/flox}$ K5-Cre mouse (Fig. 2*B*). Ki67-positive cells/basal cells were 90.5 and 40% ($p < 0.01$, $n = 4$) in *Ubc13*$^{flox/flox}$ mice and *Ubc13*$^{flox/flox}$ K5-Cre mice, respectively. Apoptotic cells/basal cells were 0 and 2.9% ($p < 0.01$, $n = 4$) in *Ubc13*$^{flox/flox}$ mice and *Ubc13*$^{flox/flox}$ K5-Cre mice, respectively. Taken together, these results indicate that Ubc13 regulates keratinocyte growth and apoptosis in mice.

Because disruption of the NF-κB pathway causes inflammation in the skin (10, 11, 14, 19), the expression of pro-inflammatory cytokines in the epidermis was studied. Real time PCR analysis revealed that TNF-α mRNA expression was decreased, whereas IL-1α expression was increased in *Ubc13*$^{flox/flox}$K5-Cre mouse epidermis (Fig. 2*C*).

Abnormal Keratinocyte Differentiation in Ubc13$^{flox/flox}$*K5-Cre Mouse Epidermis*—To analyze the differentiation status of the epidermal keratinocytes, we performed immunohistochemical analyses using skin sections treated with antibodies specific for various differentiation markers (Fig. 3). According to our data, the suprabasal keratinocytes in the epidermis of the *Ubc13*$^{flox/flox}$ K5-Cre mice expressed K14, which is normally confined to the basal layer. Loricrin is a marker of late phase keratinocyte differentiation and is normally expressed in the upper epidermis, as shown in the control mice. Loricrin expression was absent from the viable epidermal keratinocytes of the *Ubc13*$^{flox/flox}$ K5-Cre mice. K15 is a marker of the bulge area in adult mice and is also expressed at the basal cell layer in neonatal mice (20), as shown in Fig. 2. However, K15 expression was absent from the epidermis of the *Ubc13*$^{flox/flox}$ K5-Cre mice. These results indicate that keratinocyte differentiation is disrupted by the deletion of Ubc13 in keratinocytes.

Impaired Cell Growth and Spontaneous Cell Death by Ubc13 Deletion—Keratinocytes were isolated from newborn mouse epidermis and cultured for cellular function analyses. Ubc13-deficient keratinocytes had growth impairments as shown in Fig. 4*A*. Furthermore, spontaneous cell death occurred, and the dead cells were positive for TUNEL (Fig. 4*B*). Analysis of LDH release revealed that cell death began within 1 day of adherence to the culture dishes and increased over 3 days (Fig. 4*C*). Because blockade of NF-κB pathway in keratinocytes enhances susceptibility to apoptosis by TNF-α (21), the cells were treated with TNF-α. The spontaneous cell death was slightly enhanced by TNF-α but was not blocked by anti-TNF-α antibodies (Fig. 4*D*).

Next, Ubc13 was deleted in cultured keratinocytes derived from *Ubc13*$^{flox/flox}$ mice, and Ax-Cre was transfected into cultured keratinocytes from *Ubc13*$^{flox/flox}$ or *Ubc13*$^{+/+}$ mice using Ax-LacZ as a control. Ubc13 expression began to decrease at 36 h after transfection with Ax-Cre (Fig. 5*A*). The deletion of Ubc13 in the cultured keratinocytes resulted in cell death, and the dead cells were positive for TUNEL (Fig. 5*B*). Similar to Fig. 4*D*, cell death was slightly enhanced by TNF-α but was not blocked by anti-TNF-α antibodies (Fig. 5*D*). These data indicate that Ubc13 is essential for keratinocyte survival. To further

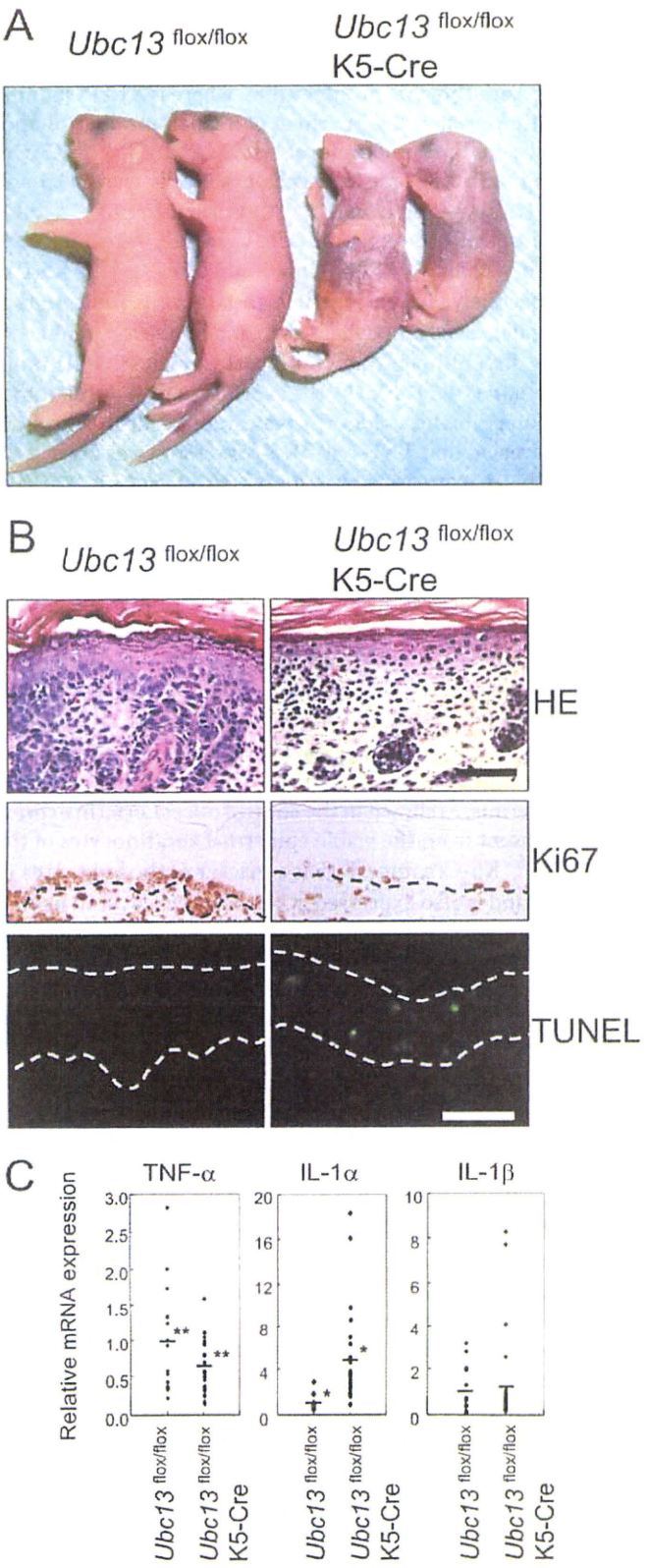

FIGURE 2. **Skin phenotypes of the *Ubc13*$^{flox/flox}$ K5-Cre mice.** *A*, appearance of the *Ubc13*$^{flox/flox}$ K5-Cre mice at postnatal day 1. The skin of the mice was abnormally shiny and smooth. *B*, histological analysis of *Ubc13*$^{flox/flox}$ K5-Cre mouse skin sections by H&E staining, Ki67 staining, and TUNEL. H&E staining showed atrophy of the epidermis in the *Ubc13*$^{flox/flox}$ K5-Cre mice. Ki67 staining showed decreased numbers of positive cells in the epidermis of the *Ubc13*$^{flox/flox}$K5-Cre mice. The epidermis also contained a few apoptotic cells as shown by H&E staining and TUNEL. The *dotted lines* indicate the basement membrane in the Ki67 section and the basement membrane and surface of the epidermis in the TUNEL section. *Ubc13*$^{flox/flox}$ represents the undeleted controls. *Scale bar*, 100 μm. *C*, mRNA expression of TNF-α, IL-1α, and IL-1β in the epidermis. Newborn mouse epidermis was separated from the dermis, and mRNA expression was analyzed by real time PCR. mRNA expression levels were normalized against GAPDH, and the mean value of *Ubc13*$^{flox/flox}$ mice was referred to as 1.0 unit. n = 17 (*Ubc13*$^{flox/flox}$ mice). n = 28 (*Ubc13*$^{flox/flox}$ K5-Cre mice). *, $p < 0.01$. **, $p < 0.05$.

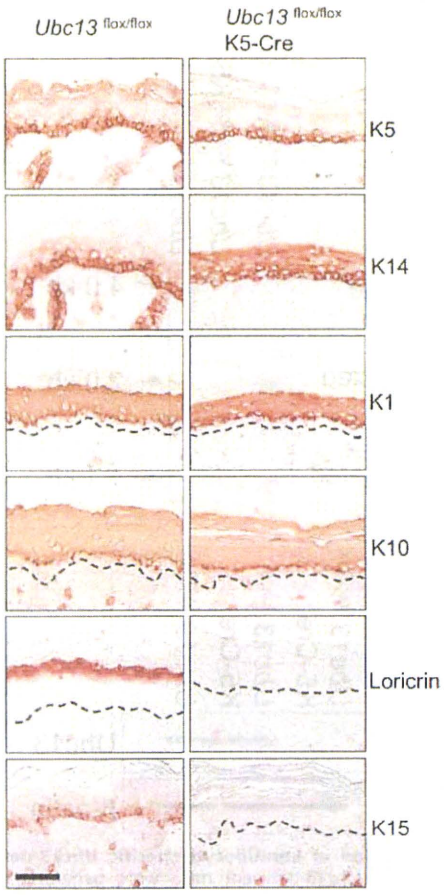

FIGURE 3. **Abnormal expression of differentiation markers in the epidermis of *Ubc13*$^{flox/flox}$K5-Cre mice.** The expression of various differentiation markers in the epidermis was analyzed immunohistochemically. The expression of K5 and K14 is normally confined to the basal cell layer. The expression of K1, K10, and loricrin marks suprabasal and late phase differentiation, whereas K15 is expressed at the basal cell layer in neonatal mouse epidermis. The *dotted lines* indicate the basement membrane. *Ubc13*$^{flox/flox}$ represents the undeleted controls. *Scale bar*, 100 μm.

study the mechanisms of spontaneous cell death, the expression of anti-apoptotic protein cIAP-2 and the activation of caspase-3 (22) were analyzed by Western blot (Fig. 5*E*). The expression of cIAP-2 was reduced by Ubc13 deletion, which was correlated with the activation of caspase-3.

Impaired Activation of p38, JNK, and NF-κB in Ubc13-deficient Keratinocytes—To study the cause of these functional defects of Ubc13-deficient keratinocytes, intracellular signals were analyzed. Because spontaneous cell death occurs, freshly isolated keratinocytes were stimulated soon after adherence to the culture dishes (Fig. 6). Neither p38 nor JNK was phosphorylated in the Ubc13-deficient keratinocytes by IL-1β or TNF-α, although both were phosphorylated within 15 min in the control keratinocytes (Fig.

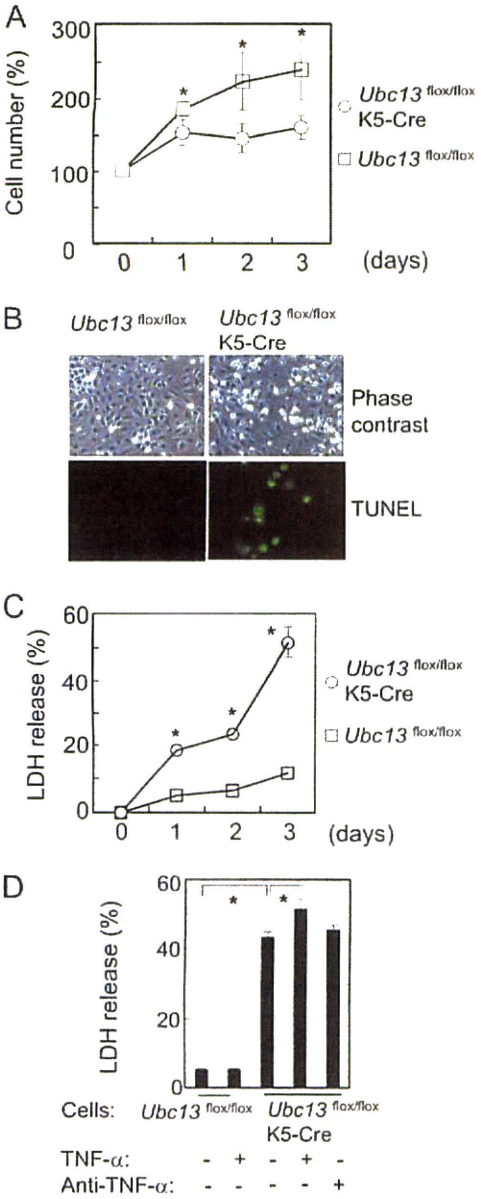

FIGURE 4. **Impaired cell growth and spontaneous cell death of *Ubc13*$^{flox/flox}$K5-Cre keratinocytes.** *A*, cell growth analysis. Freshly isolated newborn mouse keratinocytes were cultured for 3 days, and the number of cells was counted each day using a Coulter counter ($n = 6$). The number of cells at day 0 was referred to as 100%. *B*, cell morphology was examined by phase contrast microscopy, and apoptotic cells were detected using TUNEL after 2 days of culturing. *C*, cell death was quantified by measuring LDH release ($n = 6$). *D*, cytotoxic effects of TNF-α. Freshly isolated mouse keratinocytes were stimulated with mouse TNF-α (10 ng/ml) or goat anti-mouse TNF-α antibody (5 μg/ml). After 48 h, the supernatant was harvested for LDH assay. The data are expressed as the means ± S.E. ($n = 6$). *, $p < 0.01$.

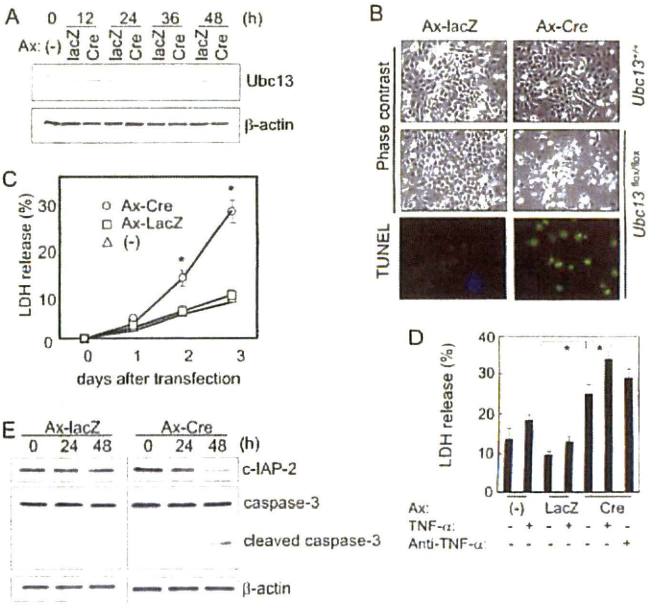

FIGURE 5. **Spontaneous cell death by deletion of Ubc13 using Ax-Cre.** Ubc13 was deleted from cultured keratinocytes derived from *Ubc13*$^{flox/flox}$ mice. Ax-Cre was transfected into the cultured keratinocytes of *Ubc13*$^{flox/flox}$ mice or *Ubc13*$^{+/+}$ mice at an multiplicity of infection of 100. Ax-LacZ was used as a control. *A*, the expression of Ubc13 in keratinocytes was analyzed by Western blotting using β-actin as an internal standard. *B*, cell morphology was examined by phase contrast microscopy, whereas apoptotic cells were detected using TUNEL at 72 h post-transfection. *C*, cell death was quantified by measuring LDH release. Ax was transfected into the cultured keratinocytes, and the culture supernatant was harvested for LDH assay at the indicated time ($n = 5$). *D*, cytotoxic effects of TNF-α. Freshly isolated *Ubc13*$^{flox/flox}$ keratinocytes were transfected with Ax at a multiplicity of infection of 100. After 24 h, the cells were stimulated with mouse TNF-α (10 ng/ml) or goat anti-mouse TNF-α antibody (5 μg/ml). After 48 h, the supernatant was harvested for use in the LDH assay ($n = 6$). The data are expressed as the means ± S.E. *, $p < 0.01$. *E*, the expression of c-IAP-2 and caspase-3 were analyzed by Western blot using β-actin as an internal standard.

6*A*). Activation of NF-κB pathway by IL-1β or TNF-α was also impaired in Ubc13-deficient keratinocytes as shown by Western blotting of IκB (Fig. 6*B*) and EMSA (Fig. 6*C*). Next, to study whether TAK1 is involved in this impaired NF-κB activation, the phosphorylation of TAK1 was analyzed. Although TAK1 was phosphorylated by IL-1β or TNF-α within 10 min in control keratinocytes, TAK1 was not phosphorylated in Ubc13-deficient keratinocytes (Fig. 6*E*). Furthermore, luciferase assay confirmed the impaired activation of NF-κB pathway (Fig. 6*D*). Because Ubc13 is a polyubiquitin-conjugating enzyme, ubiquitination of IKK-γ was studied using immunoprecipitation. As shown in Fig. 6*F*, ubiquitination of IKK-γ by IL-1β was impaired in Ubc13-deficient keratinocytes. Thus, p38, JNK, and NF-κB pathways were impaired in Ubc13-deficient keratinocytes.

Heparin-binding EGF-like growth factor (HB-EGF) is a ligand for the EGF receptor and is a potent mitogen for keratinocytes (23). We tested whether HB-EGF-induced ERK activation was also impaired in *Ubc13*$^{flox/flox}$K5-Cre keratinocytes. We found that phosphorylation of ERK by HB-EGF was not impaired (Fig. 6*G*), indicating that overall cellular signaling was not impaired in *Ubc13*$^{flox/flox}$K5-Cre keratinocytes.

DISCUSSION

In the present study, we found that Ubc13 is essential for the growth, differentiation, and survival of mouse keratinocytes. Although Ubc13 regulates NF-κB signaling, the skin phenotype of the *Ubc13*$^{flox/flox}$ K5-Cre mice was different from that of TAK1- or IKK-γ-deficient epidermis. Epidermis-specific deletion of TAK1 or IKK-γ causes inflammation, abnormal keratinocyte differentiation, and keratinocyte apoptosis in the mouse skin (14, 24). The development of similar skin phenotypes among these mice indicates the disruption of a common cascade in the keratinocytes of these mice. Although an epidermal

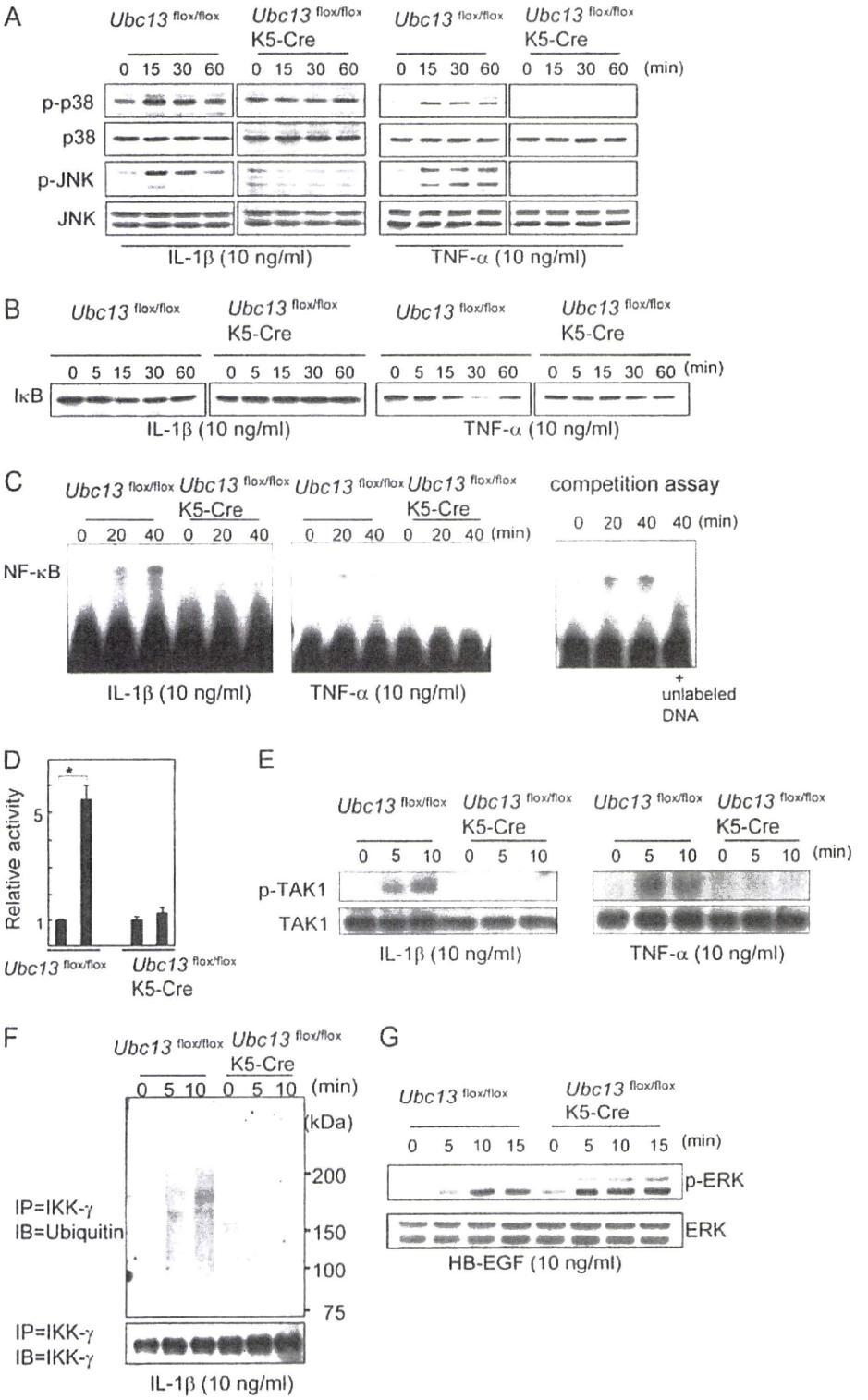

FIGURE 6. **Impaired activation of p38, JNK, and NF-κB in Ubc13-deficient keratinocytes.** Freshly isolated mouse keratinocytes were stimulated with IL-1β (10 ng/ml), TNF-α (10 ng/ml) (*A–E*), or HB-EGF (10 ng/ml) (*F*). Intracellular signals were then analyzed by Western blotting (*A*, *B*, *E*, and *G*), EMSA (*C*), luciferase assay (*D*), and immunoprecipitation (*F*, *IP*). *Ubc13*$^{flox/flox}$ represents the undeleted controls. *A*, phosphorylation of p38 and JNK (*p-p38* and *p-JNK*, respectively). p38 and JNK were used as standards. *B*, Western blotting of IκB. *C*, NF-κB activity was analyzed by EMSA. Protein-DNA complexes were separated and transferred to nylon membranes. In competition assay, *Ubc13*$^{flox/flox}$ keratinocytes were stimulated with IL-1β (10 ng/ml), and unlabeled probe (200-fold molar excess) was added to the sample of 40 min. The shift by IL-1β was prevented by the unlabeled probe, indicating that the shift was the result of specific protein-DNA interaction. *D*, luciferase assay. After transfection of pNFκB-TA-Luc, the keratinocytes were stimulated with IL-1β (10 ng/ml) for 24 h. The relative luciferase activity was calculated by normalizing to the level of *Renilla* luciferase activity. The data are expressed as the means ± S.E. *, $p < 0.01$. $n = 3$. *E*, phosphorylation of TAK1 (p-TAK1) was analyzed by Western blotting. TAK1 was the standard. *F*, ubiquitination of IKK-γ. The samples were first immunoprecipitated with anti-IKK-γ and then immunoblotted (*IB*) with anti-ubiquitin. In control cells, broad bands were detected at 5 and 10 min after the IL-1β stimulation. *G*, phosphorylation of ERK (ERK was the standard). These studies (*A–G*) were performed more than three times, and the representative data are shown.

phenotype is not apparent in TAK1- or IKK-γ-deficient mice at birth, the skin of our Ubc13-deficient mice was already abnormal at birth. The number of apoptotic cells in Ubc13-deficient epidermis was much lower than that in TAK1-deficient epidermis (14). Furthermore, the microabscesses seen in TAK1- or IKK-γ-deficient epidermis were not observed in our Ubc13-deficient mice. Although Ubc13 has been shown to regulate the NF-κB pathway in keratinocytes (Fig. 6), the phenotype produced by Ubc13 deficiency compared with that of TAK1 or IKK-γ deficiency indicates that the signaling controlled by Ubc13 is not identical to that of TAK1 or IKK-γ.

The role of Ubc13 and TAK1 in the activation of JNK, p38, and NF-κB varies by cell type and stimulus. TAK1 is indispensable for the activation of NF-κB and MAPK by TLRs, IL-1 receptor, and TNF receptor (1, 2). However, TAK1-deficient B cells can still activate NF-κB in response to B cell receptor stimulation (1). Thymocytes from TAK1-deficient mice display severely defective NF-κB activation in response to anti-CD3/CD28 stimulation (1, 25, 26); however, NF-κB activation is normal in the peripheral T cells of such animals (26). *In vivo* analyses of mice lacking Ubc13 in their B cells, myeloid cells, and embryonic fibroblasts have shown nearly normal NF-κB activation during BCR-, IL-1 receptor-, TLR, or CD40-mediated signal transduction (15), indicating that Ubc13 plays a minor role in these signaling pathways (15). Although NF-κB activation was modestly affected, JNK and p38 activation was impaired in Ubc13-deficient thymocytes (27). During IL-1 receptor-mediated signaling in these cell types, Ubc13 is more important for the activation of p38 and JNK than of NF-κB (27). However, in this study we found that in keratinocytes, Ubc13 is essential for the IL-1 and TNF-induced activation of the NF-κB, JNK, and p38 pathways. The impaired activation of these signaling pathways may cause the functional defect of Ubc13-deficient keratinocytes.

Ubc13 deficiency causes spontaneous cell death that is associated with decreased cIAP-2 and the activation of caspase-3 (Fig. 5*E*). Similarly, in TAK1-deficient keratinocytes, the expression of cIAP-2 is down-regulated and caspase-3 is activated, which causes TRAIL-induced cell death (22). These data suggest that the TAK1 deletion facilitates TRAIL-induced cell death by activating caspase through down-regulating cIAP (22). Therefore, it is most likely that decreased cIAP-2 enhanced the susceptibility to cell death in Ubc13-deficient keratinocytes, as well as TAK1. Because cIAP-2 is a target molecule of NF-κB, the down-regulation of cIAP-2 may be due to the impaired NF-κB pathway in Ubc13-deficient keratinocytes. This spontaneous cell death is enhanced slightly by TNF-α. Because TNF-α mRNA expression in the epidermis of *Ubc13*$^{flox/flox}$K5-Cre mice was decreased (Fig. 2*C*) and cell death was not blocked by anti-TNF-α antibodies (Figs. 4*D* and 5*D*), spontaneous cell death is not likely to be due to endogenous TNF-α. In studies of IKKs-deficient keratinocytes, the cells were also susceptible to TNF-induced cell death (28–30), as well as TAK1 (21). However, the effects are limited compared with the TAK1 deletion. In Ubc13-deficient keratinocytes, the cytotoxic effects of TNF are also limited (Figs. 4*D* and 5*D*). The low sensitivity to TNF in Ubc13-deficient cells may be partially due to the spontaneous cell death. Because spontaneous cell death occurs via the deletion of Ubc13 alone, susceptible cells may undergo cell death without TNF. The remaining cells may be somewhat resistant to cell death.

During embryogenesis, the NF-κB pathway is activated at the placode via binding of EdaA1 to its receptor, EdaR (31). This EdaA1/EdaR/NF-κB pathway is essential for the development of ectodermal appendages such as hair follicles, teeth, and sweat glands (32, 33). In addition, mutations of these genes can cause reduced or absent ectodermal appendages. In *Ubc13*$^{flox/flox}$ K5-Cre mice, the skin was abnormally shiny and smooth. Because the NF-κB pathway is impaired in these mice, this phenotype may be partially due to the anomaly of ectodermal appendages; however, this point should be studied further.

Because the NF-κB pathway regulates pro-inflammatory responses, the disruption of this pathway likely has a negative effect on epithelial inflammation. However, the deletion of TAK1, IKK-β, or IKK-γ results in severe inflammation (abscess formation) in the skin (10, 11, 14, 19). Similarly, a lack of NF-κB signaling caused by the conditional ablation of IKKγ or IKKα and IKKβ in the intestinal epithelium causes severe chronic intestinal inflammation in mice (34). Continuous NF-κB activation at the basal level may be required to maintain the homeostasis of the epithelium. However, the deletion of Ubc13 in epidermal keratinocytes does not cause inflammation. One possible explanation for this is the early mortality of the *Ubc13*$^{flox/flox}$ K5-Cre mice by postnatal day 2, before the occurrence of epidermal inflammation. In conclusion, Ubc13 in keratinocytes appears to be essential for maintaining epidermal integrity in mice.

Acknowledgments—We thank Teruko Tsuda and Eriko Tan for providing significant technical assistance.

REFERENCES

1. Sato, S., Sanjo, H., Takeda, K., Ninomiya-Tsuji, J., Yamamoto, M., Kawai, T., Matsumoto, K., Takeuchi, O., and Akira, S. (2005) *Nat. Immunol.* **6,** 1087–1095
2. Shim, J. H., Xiao, C., Paschal, A. E., Bailey, S. T., Rao, P., Hayden, M. S., Lee, K. Y., Bussey, C., Steckel, M., Tanaka, N., Yamada, G., Akira, S., Matsumoto, K., and Ghosh, S. (2005) *Genes Dev.* **19,** 2668–2681
3. Deng, L., Wang, C., Spencer, E., Yang, L., Braun, A., You, J., Slaughter, C., Pickart, C., and Chen, Z. J. (2000) *Cell* **103,** 351–361
4. Wang, C., Deng, L., Hong, M., Akkaraju, G. R., Inoue, J., and Chen, Z. J. (2001) *Nature* **412,** 346–351
5. Hofmann, R. M., and Pickart, C. M. (1999) *Cell* **96,** 645–653
6. Seitz, C. S., Lin, Q., Deng, H., and Khavari, P. A. (1998) *Proc. Natl. Acad. Sci. U.S.A.* **95,** 2307–2312
7. Sayama, K., Yamasaki, K., Hanakawa, Y., Shirakata, Y., Tokumaru, S., Ijuin, T., Takenawa, T., and Hashimoto, K. (2002) *J. Biol. Chem.* **277,** 40390–40396
8. Sayama, K., Hanakawa, Y., Shirakata, Y., Yamasaki, K., Sawada, Y., Sun, L., Yamanishi, K., Ichijo, H., and Hashimoto, K. (2001) *J. Biol. Chem.* **276,** 999–1004
9. Smahi, A., Courtois, G., Vabres, P., Yamaoka, S., Heuertz, S., Munnich, A., Israël, A., Heiss, N. S., Klauck, S. M., Kioschis, P., Wiemann, S., Poustka, A., Esposito, T., Bardaro, T., Gianfrancesco, F., Ciccodicola, A., D'Urso, M., Woffendin, H., Jakins, T., Donnai, D., Stewart, H., Kenwrick, S. J., Aradhya, S., Yamagata, T., Levy, M., Lewis, R. A., and Nelson, D. L. (2000) *Nature* **405,** 466–472
10. Schmidt-Supprian, M., Bloch, W., Courtois, G., Addicks, K., Israël, A., Rajewsky, K., and Pasparakis, M. (2000) *Mol. Cell* **5,** 981–992

11. Makris, C., Godfrey, V. L., Krähn-Senftleben, G., Takahashi, T., Roberts, J. L., Schwarz, T., Feng, L., Johnson, R. S., and Karin, M. (2000) *Mol. Cell* **5,** 969–979
12. Zhang, J. Y., Green, C. L., Tao, S., and Khavari, P. A. (2004) *Genes Dev.* **18,** 17–22
13. Seitz, C. S., Freiberg, R. A., Hinata, K., and Khavari, P. A. (2000) *J. Clin. Invest.* **105,** 253–260
14. Sayama, K., Hanakawa, Y., Nagai, H., Shirakata, Y., Dai, X., Hirakawa, S., Tokumaru, S., Tohyama, M., Yang, L., Sato, S., Shizuo, A., and Hashimoto, K. (2006) *J. Biol. Chem.* **281,** 22013–22020
15. Yamamoto, M., Okamoto, T., Takeda, K., Sato, S., Sanjo, H., Uematsu, S., Saitoh, T., Yamamoto, N., Sakurai, H., Ishii, K. J., Yamaoka, S., Kawai, T., Matsuura, Y., Takeuchi, O., and Akira, S. (2006) *Nat. Immunol.* **7,** 962–970
16. Takeda, J., Sano, S., Tarutani, M., Umeda, J., and Kondoh, G. (2000) *J. Dermatol. Sci.* **23,** 147–154
17. Dai, X., Sayama, K., Shirakata, Y., Tokumaru, S., Yang, L., Tohyama, M., Hirakawa, S., Hanakawa, Y., and Hashimoto, K. (2008) *J. Dermatol. Sci.* **50,** 53–60
18. Dai, X., Yamasaki, K., Shirakata, Y., Sayama, K., and Hashimoto, K. (2004) *J. Invest. Dermatol.* **123,** 1078–1085
19. Stratis, A., Pasparakis, M., Markur, D., Knaup, R., Pofahl, R., Metzger, D., Chambon, P., Krieg, T., and Haase, I. (2006) *J. Invest. Dermatol.* **126,** 614–620
20. Liu, Y., Lyle, S., Yang, Z., and Cotsarelis, G. (2003) *J. Invest. Dermatol.* **121,** 963–968
21. Omori, E., Matsumoto, K., Sanjo, H., Sato, S., Akira, S., Smart, R. C., and Ninomiya-Tsuji, J. (2006) *J. Biol. Chem.* **281,** 19610–19617
22. Morioka, S., Omori, E., Kajino, T., Kajino-Sakamoto, R., Matsumoto, K., and Ninomiya-Tsuji, J. (2009) *Oncogene* **28,** 2257–2265
23. Hashimoto, K., Higashiyama, S., Asada, H., Hashimura, E., Kobayashi, T., Sudo, K., Nakagawa, T., Damm, D., Yoshikawa, K., and Taniguchi, N. (1994) *J. Biol. Chem.* **269,** 20060–20066
24. Nenci, A., Huth, M., Funteh, A., Schmidt-Supprian, M., Bloch, W., Metzger, D., Chambon, P., Rajewsky, K., Krieg, T., Haase, I., and Pasparakis, M. (2006) *Hum. Mol. Genet.* **15,** 531–542
25. Sato, S., Sanjo, H., Tsujimura, T., Ninomiya-Tsuji, J., Yamamoto, M., Kawai, T., Takeuchi, O., and Akira, S. (2006) *Int. Immunol.* **18,** 1405–1411
26. Liu, H. H., Xie, M., Schneider, M. D., and Chen, Z. J. (2006) *Proc. Natl. Acad. Sci. U.S.A.* **103,** 11677–11682
27. Yamamoto, M., Sato, S., Saitoh, T., Sakurai, H., Uematsu, S., Kawai, T., Ishii, K. J., Takeuchi, O., and Akira, S. (2006) *J. Immunol.* **177,** 7520–7524
28. Rudolph, D., Yeh, W. C., Wakeham, A., Rudolph, B., Nallainathan, D., Potter, J., Elia, A. J., and Mak, T. W. (2000) *Genes Dev.* **14,** 854–862
29. Tanaka, M., Fuentes, M. E., Yamaguchi, K., Durnin, M. H., Dalrymple, S. A., Hardy, K. L., and Goeddel, D. V. (1999) *Immunity* **10,** 421–429
30. Li, Q., Van Antwerp, D., Mercurio, F., Lee, K. F., and Verma, I. M. (1999) *Science* **284,** 321–325
31. Schmidt-Ullrich, R., Tobin, D. J., Lenhard, D., Schneider, P., Paus, R., and Scheidereit, C. (2006) *Development* **133,** 1045–1057
32. Mikkola, M. L., and Thesleff, I. (2003) *Cytokine Growth Factor Rev.* **14,** 211–224
33. Schmidt-Ullrich, R., and Paus, R. (2005) *Bioessays* **27,** 247–261
34. Nenci, A., Becker, C., Wullaert, A., Gareus, R., van Loo, G., Danese, S., Huth, M., Nikolaev, A., Neufert, C., Madison, B., Gumucio, D., Neurath, M. F., and Pasparakis, M. (2007) *Nature* **446,** 557–561

Journal of Dermatological Science 60 (2010) 179–186

Contents lists available at ScienceDirect

Journal of Dermatological Science

journal homepage: www.elsevier.com/jds

PPARγ mediates innate immunity by regulating the 1α,25-dihydroxyvitamin D3 induced hBD-3 and cathelicidin in human keratinocytes

Xiuju Dai, Koji Sayama *, Mikiko Tohyama, Yuji Shirakata, Yasushi Hanakawa, Sho Tokumaru, Lujun Yang, Satoshi Hirakawa, Koji Hashimoto

Department of Dermatology, Ehime University School of Medicine, Ehime, Japan

ARTICLE INFO

Article history:
Received 14 May 2010
Received in revised form 17 September 2010
Accepted 21 September 2010

Keywords:
Keratinocyte
1α,25-Dihydroxyvitamin D3
PPARγ
hBD-3
Cathelicidin
AP-1

ABSTRACT

Background: Production of antimicrobial peptides (AMPs) is the primary mechanism by which skin innate immunity protects against infection. Hormonally active vitamin D3 (1α,25-dihydroxyvitamin D3; $1,25D_3$) is a vital regulator of skin innate immunity, and has been shown to increase the expression and function of AMPs.

Objective: PPARγ is a ligand-activated nuclear receptor and plays a role in keratinocyte differentiation and cutaneous homeostasis. In this study, we investigate whether $1,25D_3$-activated PPARγ signaling regulates AMP expression in keratinocytes.

Methods: Subconfluent keratinocytes were treated with $1,25D_3$ for the indicated times. The mRNA and protein levels of AMPs were detected by RT-PCR and Western blot, and the DNA binding activation of PPARγ, VDRE and AP-1 was investigated by EMSA. To examine the role of PPARγ, the recombinant adenovirus carrying a dominant-negative form of PPARγ (dn-PPARγ) was constructed and transfected into keratinocytes.

Results: We show here that $1,25D_3$ significantly enhances hBD-3 and cathelicidin expression in keratinocytes. Expression of dn-PPARγ did not affect binding to the vitamin D-responsive element (VDRE), which is crucial for cathelicidin induction by VD3; however, it did decrease $1,25D_3$ induction of both hBD-3 and cathelicidin. Inhibition of the p38, ERK, and JNK signaling pathways blocked hBD-3 expression, whereas only p38 inhibition suppressed cathelicidin induction. dn-PPARγ had no effect on ERK and JNK activity, but inhibited p38 phosphorylation and suppressed $1,25D_3$-induced AP-1 activation via effects on Fra1 and c-Fos proteins.

Conclusions: In conclusion, PPARγ regulates the $1,25D_3$-induced hBD-3 and cathelicidin expression in keratinocytes through the regulation of AP-1 and p38 activity.

1. Introduction

Epidermal keratinocytes differentiate to form a multilayered epidermis that is the primary barrier between the body and the outer environment. Despite the constant exposure of the epidermis to a wide varied of microbial pathogens, skin infections are relatively rare. The synthesis and secretion of AMPs by epithelia is recognized as an important mechanism for host defense. As effectors of innate immunity, AMPs directly kill a broad spectrum of microbes, including Gram-positive and Gram-negative bacteria as well as fungi and certain viruses. They also trigger and coordinate multiple components of the innate and adaptive immune system [1,2].

The major AMPs found in humans are cathelicidins and defensins [1,3]. Defensins are classified as α- or β-defensins based on the distribution of the cysteines and disulfide bonds. Whereas most α-defensins are produced by neutrophils, human β-defensins (hBDs) are generated mainly by epithelial tissues including the skin and respiratory tract. The three best-characterized hBDs, hBD-1, hBD-2, and hBD-3, have been detected in human skin and cultured keratinocytes. hBD-1 expression is primarily constitutive, whereas hBD-2 and hBD-3 expression is induced by cytokines, as well as growth factors, various microorganisms, and other microbial products [2,3]. In addition to hBDs, the skin epithelium also generates cathelicidins [1,2], a family of antimicrobial peptides with a highly conserved N-terminal cathelin domain and a C-terminal cationic antimicrobial domain that is

Abbreviations: AMP, antimicrobial peptide; $1,25D_3$, 1α,25-dihydroxyvitamin D3; Ax, adenovirus vector; PPAR, peroxisome proliferator-activated receptor; VDR, vitamin D receptor; VDRE, vitamin D response elements; hBD, human β-defensin.

* Corresponding author at: Department of Dermatology, Ehime University Graduate School of Medicine, Ehime 791-0295, Japan. Tel.: +81 89 960 5350; fax: +81 89 960 5352.

E-mail addresses: daixiuju@m.ehime-u.ac.jp (X. Dai), sayama@m.ehime-u.ac.jp (K. Sayama).

0923-1811/$36.00 © 2010 Japanese Society for Investigative Dermatology. Published by Elsevier Ireland Ltd. All rights reserved.
doi:10.1016/j.jdermsci.2010.09.008

activated following cleavage. Although many cathelicidins have been identified in mammals, only one cathelicidin AMP, also known as hCAP18/LL-37/FALL-39, is present in humans [1,2]. The biological relevance of these AMPs in skin has been illustrated by several clinical correlations [1,2,4]. Thus, patients with atopic dermatitis lack the appropriate AMPs and are more susceptible to skin infections, whereas psoriasis patients, who rarely develop bacterial skin infections, show high epidermal AMP expression. In spite of these, the molecular mechanisms of AMP regulation in keratinocytes are poorly understood.

$1,25D_3$, the hormonally active form of vitamin D3, decreases proliferation and increases terminal differentiation of keratinocytes, and also acts as a regulator of skin immunity. In skin injury, activated vitamin D3 metabolism leads to rapid induction of genes important for microbial recognition and antimicrobial defense [5]. The genomic effects of $1,25D_3$ are mediated by its nuclear hormone receptor, the vitamin D receptor (VDR). After activation by $1,25D_3$, the VDR binds to consensus sequences known as VDREs in the promoter region of target genes, including cathelicidin and hBD-2 [6]. $1,25D_3$ induces cathelicidin and/or hBD-2 expression in keratinocytes and myeloid cells [6–9], and strengthens cell antimicrobial activity [6–8]. Topical treatment of human skin with $1,25D_3$ also enhance cathelicidin peptide expression [8], suggesting a role of vitamin D3 or its analogs as topical immune modulators [5].

PPARγ signaling regulates keratinocyte differentiation and cutaneous homeostasis, in a manner similar to other nuclear hormones such as glucocorticoids, retinoids, and vitamin D [10–12]. We have previously showed that suspension culture and $1,25D_3$ treatment of keratinocytes increases PPARγ expression and activity, which contributes to involucrin expression and keratinocyte differentiation [13,14]. Keratinocyte differentiation often upregulates innate immunity [15], but the function of PPARγ in skin innate immunity remains unclear. We investigated if $1,25D_3$-activated PPARγ signaling regulates AMP expression in keratinocytes, and demonstrated an important role for PPARγ signaling in the regulation of keratinocyte immune responses.

2. Materials and methods

2.1. Keratinocyte culture

Primary normal human keratinocytes were isolated from surgically discarded neonatal skin samples. This study was conducted according to principles of the Declaration of Helsinki, and all procedures that involved human subjects received prior approval from the ethics committee at the Ehime University School of Medicine. Written consent was provided by patient guardians before experiments were initiated. Normal human keratinocytes were cultured in MCDB153 medium as described previously [14].

2.2. Adenovirus vector construction and infection

The pcDNA3 expression vectors expressing flag-tagged wild-type (wt) PPARγ and flag-tagged L468A/E471A PPARγ (dn-PPARγ) were gifts from Professor K. Chatterjee (University of Cambridge, UK). The double-mutant form of PPARγ shows impaired transcriptional activity, silences basal transcription, and is a potent dominant-negative inhibitor of wild-type PPARγ activity [16]. An adenovirus vector (Ax) containing wt-PPARγ or dn-PPARγ was generated and transfected into keratinocytes as described previously [13]. Ax1W was used as the control vector to control for effects of Ax itself.

2.3. RNA preparation and real-time RT-PCR

Total RNA from cultured cells was isolated using Isogen (Nippon Gene, Tokyo, Japan). Real-time RT-PCR was performed and analyzed in an ABI PRISM 7700 sequence detector (Applied Biosystems, Branchburg, NJ). The primers and probes used for hBD-3 (forward: 5′-TCAGCTGACTTCCAAAGGA-3′, reverse: 5′-TCAGCTGACTTCCAAAGGA-3′, probe: 5′-AACAGATCGGCAAGTGCTCGACGC-3′) and cathelicidin (forward: 5′-CACAGCAGTCACCAGAGGATTG-3′, reverse: 5′-GGCCTGGTTGAGGGTCACT-3′, probe: 5′-GGCCTGGTTGAGGGTCACT-3′) were selected using the Primer Express software (Applied Biosystems). The primers and probe for GAPDH were obtained from Applied Biosystems. RNA analysis was carried out using the TaqMan RT-PCR Master Mix Reagent Kit (Applied Biosystems), following the suggested protocol. The level of target gene expression was normalized to GAPDH and is reported as the change relative to control.

2.4. Protein preparation and Western blot analysis

Keratinocytes were harvested at specific times after treatment and whole cell lysates were extracted. Twenty micrograms of protein was separated by SDS-PAGE and transferred to polyvinylidene difluoride membranes. Analyses were performed using a Vistra ECF Kit (Amersham Biosciences, Arlington Heights, IL), and membranes were then scanned using a FluorolImager (Molecular Dynamics, Sunnyvale, CA). The following antibodies were used for Western blotting: goat anti-β-actin (Santa Cruz Biotechnology, Santa Cruz, CA), rabbit anti-cathelicidin (Innovagen, Lund, Sweden), mouse anti-hBD-3 (Alpha Diagnostics, San Antonio, TX), rabbit anti-VDR, mouse anti-PPARγ and rabbit anti-Fra1 (Santa Cruz Biotechnology), as well as rabbit antibodies against c-Fos, p38, phospho-p38, phospho-ERK, and phospho-JNK (Cell Signaling Technology, Beverly, MA). The nuclear lysates used for Western blotting were extracted as described previously [17].

2.5. Preparation of nuclear extracts and electrophoretic mobility shift assays (EMSAs)

Nuclear proteins were isolated, and the EMSA was performed as described previously [13] using a Light Shift® Chemiluminescent EMSA Kit (Pierce, Rockford, IL) according to the manufacturer's instructions. The oligonucleotide probe sets (biotin-labeled and unlabeled probes) specific for PPARγ [13], VDRE and AP-1 [14] were obtained from Panomics (Redwood City, CA). Protein–DNA complexes were separated and transferred to Biodyne® B nylon membranes (Pierce). The biotin-labeled molecules in the membranes were detected using a Chemiluminescent Nucleic Acid Detection Module (Pierce) and exposed to X-ray film [13].

2.6. Chemicals

$1,25D_3$ was a generous gift from Teijin Pharmaceutical Co. Ltd. (Tokyo, Japan). Different concentrations of $1,25D_3$ or an equal volume of EtOH (vehicle) were added to cultures. SB203580, PD98059, and SP600125 were purchased from Calbiochem-Novabiochem International Co. (San Diego, CA) and dissolved in DMSO at 2, 30, and 20 mM, respectively, as stock solutions, and used at final concentrations of 1, 30 and 10 μM, respectively.

2.7. Statistical analysis

At least three independent experiments were performed, with similar results. One representative experiment is shown in each figure. The relative mRNA expression was expressed as the mean ± SD ($n > 3$). Statistical significance was determined using Student's paired t-tests. Differences were considered statistically significant at $p < 0.05$ and indicated as $^*p < 0.05$ in the figures.